amyloid enzyme-linked immunosorbent assay kit (WAKO, Osaka, Japan). Cell surface biotinylation was performed using Pierce cell surface protein isolation kit (Pierce) according to the manufacturer's instruction.

RESULTS

Anti-NCT Intrabody Decreases the Expression Levels of NCT and Suppresses the γ-Secretase Activity—Budded baculovirus from Sf9 cells infected with recombinant virus displays the recombinant proteins on its virion membrane (30, 40). Thus, budded baculovirus can be used as an optimal immunogen to generate monoclonal antibodies against the membrane proteins. Using this technology, we have generated a monoclonal antibody A5201A that specifically binds to NCT ECD. A5201A showed specific binding ability to V5-tagged NCT ECD in a similar manner to anti-V5 antibody, whereas an irrelevant IgG exhibited no reactivity (Fig. 1). Next, we generated two intrabodies based on A5201A, named 5201C and 5201F. Both intrabodies consist of light and heavy chain variable regions that were cloned from hybridoma cells producing A5201A, conjugated with three GGGGS pentapeptide repeats as a linker by PCR. Each cDNA was cloned into a pSecTag2C vector, which enables the targeting of the intrabodies into the lumen by the Igκ leader sequence and detection with c-*myc* tag attached to the C terminus (Fig. 2*A*). 5201C and 5201F harbored a difference only in the light chain variable region sequences, whereas the heavy chain variable region sequences were totally identical. As NS-1 cells, the mouse myeloma cells used for the generation of the hybridoma (40) endogenously express κ light chain gene, one of the two light chain sequences might be derived from NS-1 cells.

We then generated HEK293 cell lines stably expressing 5201C or 5201F (Fig. 2*B*, supplemental Fig. S1). Immunoblot analysis revealed that both intrabodies were expressed intracellularly as a ~36-kDa protein and secreted into culture media. Intriguingly, the expression levels of NCT, especially that of mature NCT, were markedly reduced in 5201F-expressing cell lines, and the remaining "mature-like" NCT showed slightly longer migration on SDS-PAGE than that of mock- or 5201C-expressing cells. Hereafter, we refer to this mature-like NCT of ~115 kDa observed in 5201F-expressing cells as NCT*. Moreover, the protein levels of other components of the γ-secretase complex, *i.e.* PS1, APH-1aL, and PEN-2, were also decreased in 5201F-expressing cells. In contrast, none of the γ-secretase components was affected in 5201C-expressing cells. Next, we examined whether the intrinsic γ-secretase activity was affected in the intrabody-expressing cells by *in vitro* assay using an APP-based recombinant substrate (3, 38). We then normalized the activity against the levels of PS1 CTF to measure the specific activity per active complex (20). 5201F-expressing cells showed significant reduction in the Aβ-generating activities (for Aβ40, 34.5% (#2) and 23.9% (#4) compared with that of mock cells; for Aβ42, 21.3% (#2) and 39.4% (#4)) (Fig. 2*C*). These results suggest that the overexpression of intrabody 5201F, but not 5201C, reduces the steady-state expression levels as well as the intrinsic activity of the γ-secretase complex.

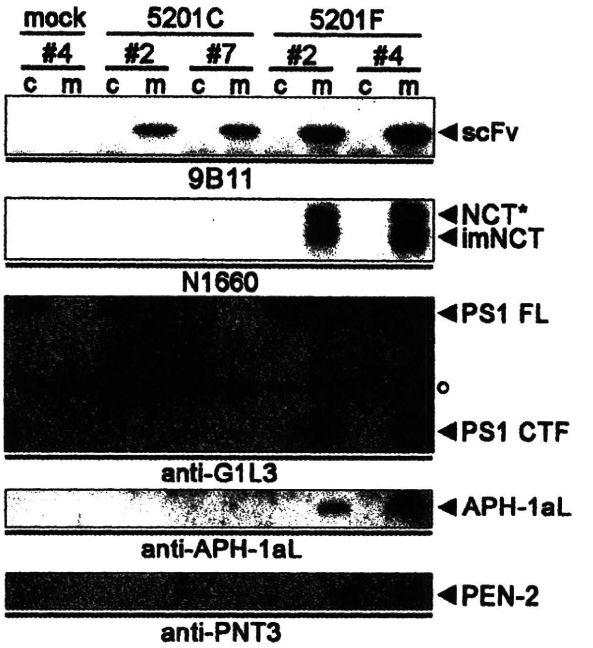

FIGURE 3. **Incorporation of 5201F into the γ-secretase complex.** Co-immunoprecipitation analysis of 1% CHAPSO-solubilized fractions from intrabody-expressing stable HEK293 cells with control IgG (*c*) or anti-c-*myc* antibody 9B11 (*m*). Immunoprecipitates were analyzed by immunoblotting with each antibody indicated *below the panel*. The *white circle* indicates the immunoglobulin chain. *imNCT* immature NCT.

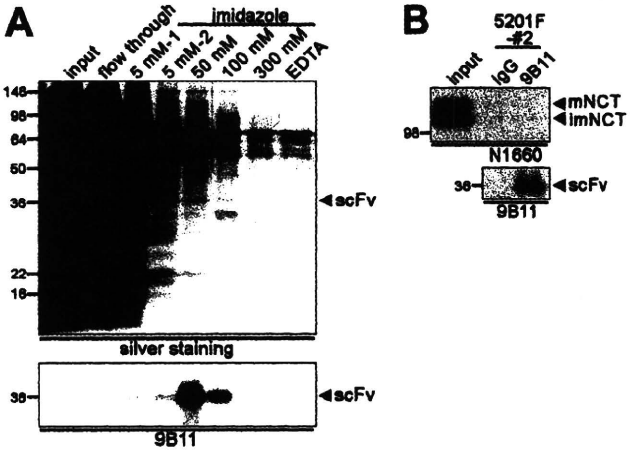

FIGURE 4. **Secreted 5201F failed to bind NCT.** *A*, culture media of 5201F-expressing cells were applied to a nickel chelating column, and the bound proteins were eluted with stepwise increased concentrations of imidazole and EDTA. Eluates were dialyzed against phosphate-buffered saline and then analyzed with silver staining (*upper panel*) and immunoblotting with anti-c-*myc* antibody 9B11 antibody (*lower panel*). *B*, partially purified secreted scFv from the 100 mM imidazole fraction in *A* was mixed with 1% CHAPSO-solubilized HEK293 cell lysates and immunoprecipitated with control IgG or anti-c-*myc* 9B11 antibody. Immunoprecipitates were analyzed by immunoblotting using each antibody indicated *below the panels*. Note that secreted scFv failed to bind with endogenous NCT. *mNCT* and *imNCT* represent mature and immature NCT, respectively.

5201F, but Not 5201C, Binds to NCT ECD in the γ-Secretase Assembly Process—We then examined the interactions of the intrabodies with the γ-secretase complex by immunoprecipitation analysis. NCT* as well as immature NCT were co-precipitated with intrabody only from 5201F-expressing cells (Fig. 3).

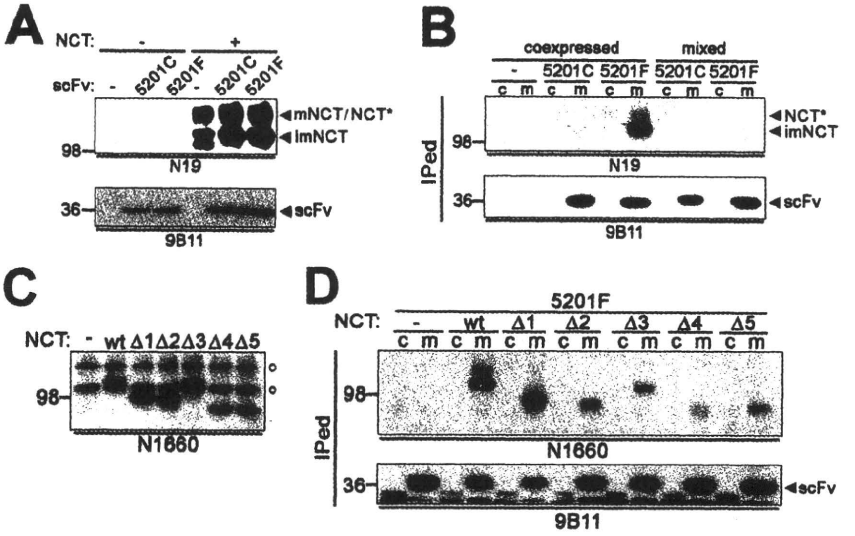

FIGURE 5. **Direct binding of intracellular 5201F to NCT.** *A*, immunoblotting of the NKO cells overexpressing intrabodies with or without human NCT. *mNCT* and *imNCT* represent mature and immature NCT, respectively. *B*, immunoprecipitation (*IPed*) of 1% CHAPSO-solubilized NKO cells with control IgG (*c*) or anti-c-*myc* antibody 9B11 (*m*). *Coexpressed* samples were the lysates from NKO cells coexpressing intrabodies and human NCT. *Mixed* samples were the mixture of the lysate from NKO cells either expressing intrabodies or NCT. *C*, immunoblotting of the NKO cells coexpressing the deletion mutant of human NCT together with 5201F. *White circles* indicate nonspecific proteins appeared in NKO cells. *D*, immunoprecipitation of 1% CHAPSO-solubilized NKO cells in *C* with anti-c-*myc* antibody 9B11.

All γ-secretase components were also detected in the immunoprecipitates with 5201F. These data suggest that 5201F directly interacts with NCT and that 5201F-bound NCT is incorporated into the γ-secretase complex. Unexpectedly, however, 5201F purified from conditioned media failed to pull down NCT from HEK cell lysates (Fig. 4). Then, we transiently expressed intrabody in the presence or absence of human NCT in NKO cells (32) and performed the immunoprecipitation analysis using mixed lysates. The coexpressed 5201F precipitated NCT polypeptides, whereas the intrabody in NKO cells failed to interact with the independently expressed NCT (Fig. 5, *A* and *B*), suggesting that the intrabody 5201F is incorporated into the γ-secretase complex during its assembly process. Moreover, significant reduction of mature NCT was observed in stable NKO cells coexpressing 5201F and human NCT in a similar manner to that in HEK293 cells expressing 5201F, suggesting that 5201F was able to form NCT* in NKO cells (supplementary Fig. S2). Next, we analyzed the location of the epitope of the intrabody 5201F using systematically deleted constructs (NCT/Δ1-Δ5) of NCT ECD (17) in NKO cells. Previous results have suggested that these deletion constructs encode loss-of-function mutant forms of NCT. Although 5201F bound to all deletion NCT mutants, the immunoreactivities against NCT/Δ2, Δ3, Δ4, and Δ5 were significantly reduced, suggesting that 5201F directly recognizes a broad region in NCT ECD irrespective of the formation of functional γ-secretase complex (Fig. 5, *C* and *D*). Collectively, these results suggest that the intracellularly expressed scFv 5201F directly targets the nascent or newly synthesized NCT polypeptides during the biosynthetic pathway and is incorporated into the γ-secretase complex.

Binding of 5201F Prevents the Glycosyl and the Structural Maturation of NCT—During the maturation process of the γ-secretase complex, NCT ECD undergoes a complex glycosylation and a conformational change to acquire trypsin resistance along with the trafficking from ER to the cell surface (11–17). To investigate the molecular mechanism by which the binding of 5201F decreased the expression levels of NCT as well as of the γ-secretase components, we biochemically characterized NCT*. In the metabolic labeling experiment, NCT was synthesized as ~110-kDa core-glycosylated intermediate form of polypeptides at 0 h of chase (Fig. 6*A*) (11, 13). The levels of NCT core polypeptides were comparable among the stable cell lines, indicating that the overexpression of intrabodies had no effect on the translation efficiency of NCT. Three hours after synthesis, measurable levels of NCT were converted to the 100 kDa immature form by trimming of glucose and mannose in the ER. Then these NCT matured into the complex glycosylated forms that exhibited retarded migration at 120 kDa. This mature NCT was long-lived, and significant levels of labeled mature NCT were still present 48 h after labeling as previously reported (11). In 5201F-expressing cells, however, the levels of immature NCT were relatively low at 3 h of chase and the conversion to NCT* was completed within 6 h. Moreover, 48 h after synthesis, NCT* was still present but clearly lesser in amount compared with that of mature NCT in mock- or 5201C-expressing cells, suggesting that the binding of 5201F caused rapid and inappropriate maturation of NCT polypeptides and rendered the NCT* unstable.

Next we examined the glycosylation state of NCT* by Endo H digestion. Mature NCT in mock- or 5201C-expressing cells was Endo H-resistant and migrated at ~120 kDa in SDS-PAGE, whereas immature NCT was completely deglycosylated as previously described (Fig. 6*B*) (11–17). Unexpectedly, NCT* showed Endo H resistance, too. Moreover, cell surface biotinylation experiments revealed that mature NCT* was displayed on the plasma membrane in a similar manner to the mature NCT of the control cell lines (Fig. 6*C*). The levels of PS1 N-terminal fragment in mock- and 5201F-expressing cells were almost comparable (supplemental Fig. S3), suggesting that the steady-state level of the γ-secretase complex containing 5201F on the cell surface is not significantly altered. Finally, we examined the trypsin resistance of NCT*. As previously described (17), substantial levels of mature NCT in mock- or 5201C-expressing cells remained intact after 30-min of incubation with trypsin, whereas immature NCT was completely digested (Fig. 6*D*). In contrast, in 5201F-expressing cells, NCT* was completely digested by trypsin in a similar manner to that

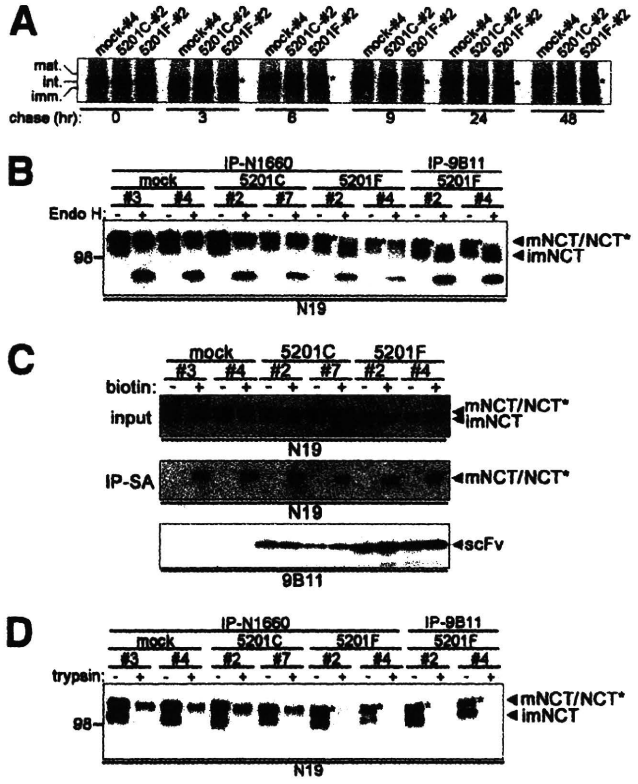

FIGURE 6. **Characterization of NCT* observed in 5201F-expressing cells.** *A*, metabolic labeling of stable HEK293 cells. Cells were pulse-labeled with [^{35}S]methionine and cysteine for 30 min and chased for indicated time periods. Lysates were immunoprecipitated with anti-NCT C terminus antibody N1660 and analyzed. NCT* is denoted by *asterisks*. *mat.*, mature; *imm.*, immature; *int.*, intermediate. *B*, immunoblotting of NCT polypeptides digested by Endo H. Immunoprecipitates (*IP*) with anti-NCT C terminus antibody N1660 or anti-c-*myc* antibody 9B11 were incubated with (+) or without (−) Endo H and analyzed by immunoblotting with anti-NCT N terminus antibody N19. *C*, cell surface biotinylation of HEK293 cells. Cell lysates (*input*) as well as biotinylated proteins (*IP-SA*) were analyzed using each antibody indicated *below the panels*. *D*, trypsin digestion of NCT polypeptides. Immunoprecipitates with anti-NCT C terminus antibody N1660 or anti-c-*myc* antibody 9B11 were incubated with (+) or without (−) 100 μg/ml trypsin and analyzed as in *B*.

of immature NCT. These results indicate that the binding of 5201F partially prevents the conformational as well as glycosyl maturation of NCT.

Conformational Maturation of NCT Is Required for the Stabilization of the γ-Secretase Complex—Large deletions in NCT ECD caused total loss of function of NCT (*i.e.* NCT/Δ1-Δ5) by failure in acquiring conformational maturation (10, 17). However, it is difficult to analyze the effect of the conformational defects in NCT ECD using these mutants because of the nature of deletion mutation; in fact, the overexpression of NCT/Δ312 in NKO cells completely failed to generate mature NCT (Refs. 10, 14, and 17; see below). To test whether a "partial" conformational defect of NCT affects the intrinsic γ-secretase activity, we introduced amino acid substitutions into the highly conserved residues at the juxtamembrane region of NCT ECD (*i.e.* Trp-648, Glu-650, and Ser-651 to alanine; 648ATAA), which play an important functional role in the γ-secretase complex formation (Fig. 7*A*) (41). The overexpression of NCT/648ATAA in NKO cells partially rescued the generation of mature NCT and PS1 fragments (Fig. 7*B*). Cycloheximide treatment caused rapid degradation of PS1 CTF in NCT/648ATAA-overexpressing cells, whereas PS1 CTF in cells expressing wild-type NCT was stable as previously reported (42), indicating that the reconstituted γ-secretase complex by NCT/648ATAA mutant is unstable (Fig. 7*C*). The trypsin digestion experiment revealed that mature NCT/648ATAA was readily degraded, suggesting that mutant NCT failed to acquire the conformational maturation, thereby causing the instability of the γ-secretase complex (Fig. 7*D*). The *de novo* Aβ generating activity in NCT/648ATAA-expressing NKO cells was also decreased (66.3% of that in wild-type human NCT-expressing cells). Notably, however, the *de novo* activity normalized by PS1 CTF levels in cells expressing NCT/648ATAA was not reduced compared with that in wild-type human NCT-expressing cells (Fig. 7*E*). These data suggest that the defect in the conformational maturation of NCT ECD caused the decrease in the total Aβ generating activity by loss of stability of the functional γ-secretase complexes, whereas the intrinsic activity of the enzyme was unaltered.

Glucose Trimming in ER Is Required for the Intrinsic Activity of the γ-Secretase Complex—*N*-Glycosylated proteins are folded by ER-resident chaperones (e.g., calnexin (CNX) or calreticulin) that recognize a monoglucose on unfolded polypeptides (43, 44). During the folding process, the transfer and the trimming of glucose are executed by the ER-resident glucosyltransferase and glucosidase, respectively. Thus, unfolded, but still glucose-attached proteins are captured by CNX to be folded; this process is called "the CNX cycle." To test the possibility that the CNX cycle is involved in the maturation of NCT, the immunoprecipitation analysis was performed. We confirmed the association of CNX and NCT as previously described (Fig. 8*A*) (45). Moreover, this interaction was significantly reduced by the overexpression of 5201F (Fig. 8*B*), suggesting that the glucose trimming and/or the CNX cycle would be inhibited by the scFv. Castanospermine (CST) is an α1,2-glucosidase inhibitor that causes the inhibition of interaction between *N*-linked glycoproteins and CNX (46, 47). The CST treatment caused the accumulation of aberrant NCT polypeptides, which presumably represent the glucosylated form of NCT (glucoNCT) (Fig. 9*A*). Intriguingly, glucoNCT showed a similar molecular weight to that of NCT* and acquired the Endo H resistance (Fig. 9*B*). In contrast, the levels of the γ-secretase components and the trypsin resistance of NCT were unaffected, suggesting that the glucose trimming is dispensable for the proper folding of NCT and the trafficking of the stable γ-secretase complex (Fig. 9, *A* and *C*). However, specific *de novo* Aβ generating activity normalized by PS1 CTF levels in CST-treated cell membrane was significantly decreased to a similar extent to that in 5201F-expressing cells (for Aβ40, 32.0% compared with that of mock-treated cells; for Aβ42, 33.4%) (Fig. 9*D*). These data indicate that the proper glucose trimming of NCT ECD accompanied by the CNX cycle is required for the intrinsic γ-secretase activity but not for the formation of the stable enzyme complex. Taken together, the binding of scFv 5201F has detrimental effects both on the

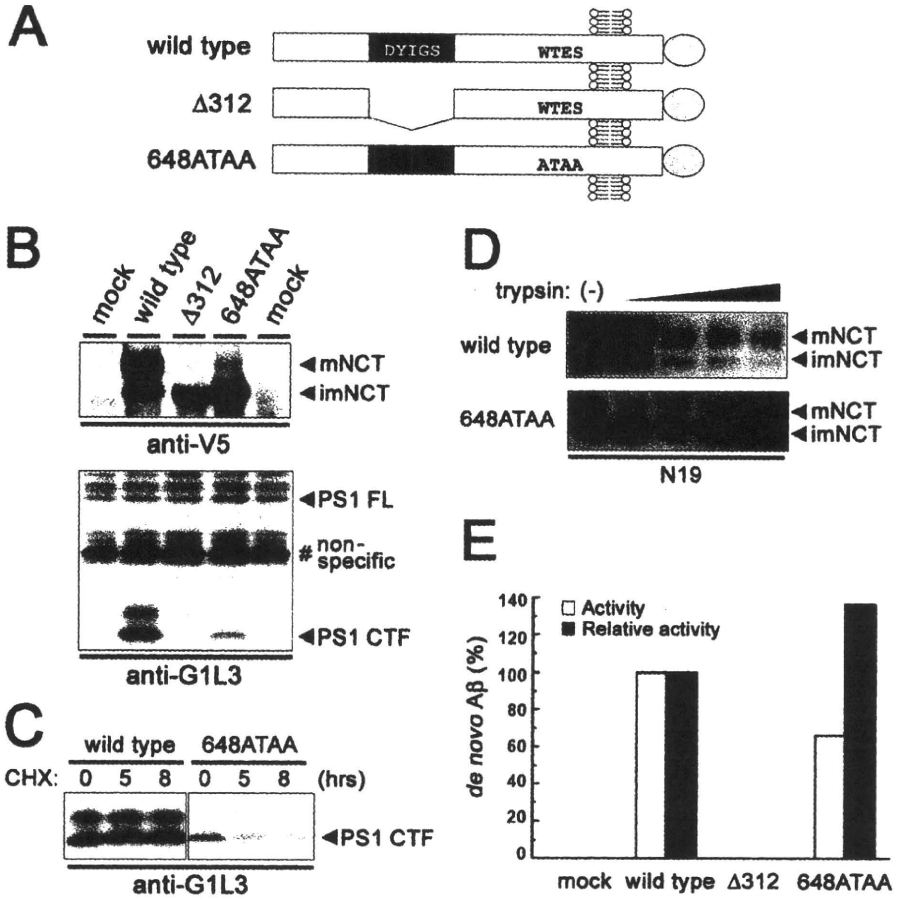

FIGURE 7. **The role of conformational maturation of NCT in the γ-secretase activity.** *A*, schematic depiction of NCT mutants analyzed in this experiment. The *black box* indicates highly conserved region containing DYIGS motif (312–369). The C-terminal V5 tag is indicated by *shaded circle*. *B*, immunoblot analysis of wild-type and mutant NCT-expressing NKO cell lysates. *mNCT* and *imNCT* represent mature and immature NCT, respectively. *C*, immunoblot analysis of wild-type and mutant NCT expressing NKO cells treated with cycloheximide (*CHX*) as previously reported. Lysates were prepared after cycloheximide treatment for various incubation times as indicated *above the lanes*. *D*, trypsin digestion of wild- type or mutant NCT polypeptides. *E*, *de novo* γ-secretase activity of the mutant NCT-expressing cells measured by *in vitro* assay. *White bars* indicate the proteolytic activity in the solubilized membrane containing equal protein amounts. *Black bars* denote the relative activity normalized by the γ-secretase levels, which were assessed by densitometric analysis of PS1 CTF on immunoblotting.

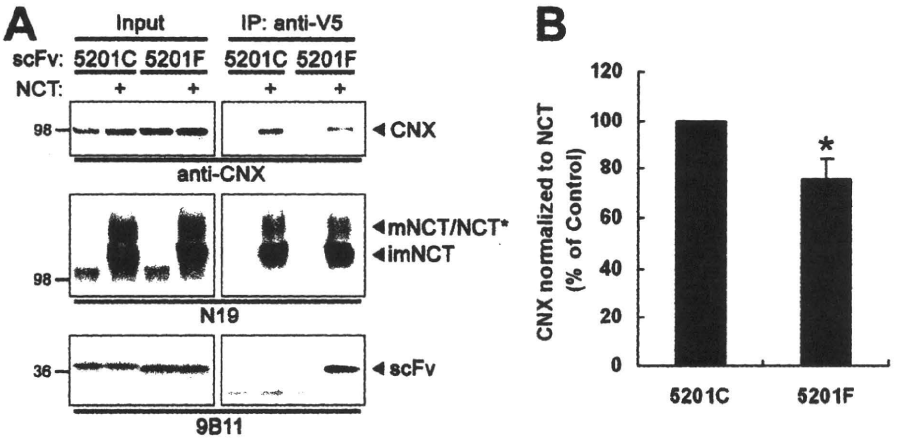

FIGURE 8. **Interaction of CNX and NCT.** *A*, immunoprecipitation (*IP*) analysis of NKO cell lysate transiently coexpressing human NCT and intrabodies. Immunoreactivities of NCT-bound CNX were quantified and normalized by the amount of total NCT in *B* ($n = 7$; *, $p < 0.05$, Student's *t* test).

conformational maturation and the glucose trimming of NCT ECD, thereby causing the destabilization and the loss of the enzymatic activity of the γ-secretase complex, respectively.

DISCUSSION

Recently, much attention is being focused on the use of scFv fragments as intrabodies. Intrabodies have been used for phenotypic knock-out of endogenous target proteins by several different strategies. In this study we generated two intrabodies by using an anti-NCT ECD monoclonal antibody A5201A as a template. Biochemical analyses revealed that the specific binding of 5201F on NCT ECD inhibited the conformational change and the proper glycosylation of NCT, thereby causing the destabilization of the γ-secretase complex and the loss of proteolytic activity. Our results suggest that the functional maturation of NCT ECD regulates the proper trafficking, stability, and the specific activity of the γ-secretase complex.

γ-Secretase is an unusually stable protease that has >24 h of half-life in mammalian cells (42). Biochemical studies have shown that NCT forms a subcomplex with APH-1 within the biosynthetic pathway (48) and functions as a stabilizing cofactor as well as a substrate receptor for the γ-secretase complex (19, 20). The assembly of the γ-secretase complex occurs in the ER (49, 50), and only "functionally" assembled γ-secretase is subsequently sorted out to the Golgi apparatus in Rer1- and COPII-regulated manners (5, 51–53). However, the molecular information on the quality control of a prefunctional γ-secretase complex in the ER remains unknown. Here, we showed that the overexpression of 5201F caused an inappropriate glycosylation and prevented NCT polypeptides from acquiring the trypsin resistance, thereby causing the phenotypic "knock-out" of the γ-secretase components. Notably, we found that 5201F accelerated the inappropriate

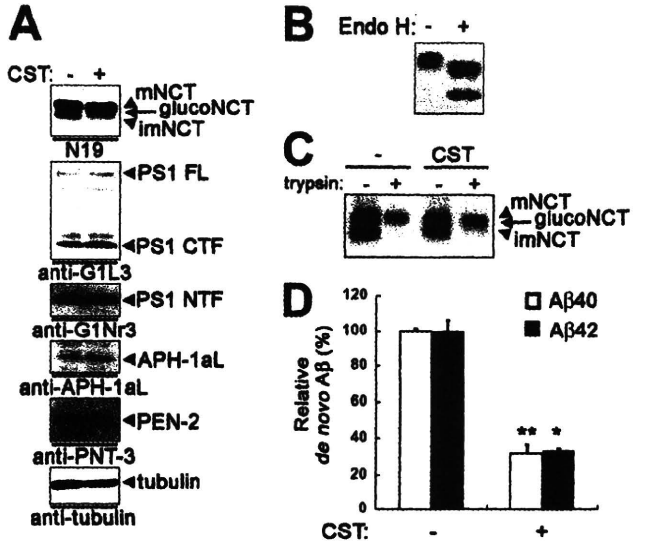

FIGURE 9. **The role of glucose trimming in NCT maturation and the γ-secretase activity.** *A*, immunoblot analysis of CST-treated HEK293 cell lysates. Note that CST treatment caused the accumulation of aberrant molecular weight NCT (*glucoNCT*). *mNCT* and *imNCT* represent mature and immature NCT, respectively. *NTF*, N-terminal fragment. *B*, Endo H and *C*, trypsin digestion of glucoNCT accumulated by CST treatment. *D*, specific γ-secretase activity of the CST-treated HEK293 cells analyzed by *in vitro* assay as in Fig. 1*C* ($n = 3$; *, $p < 0.01$, Student's *t* test).

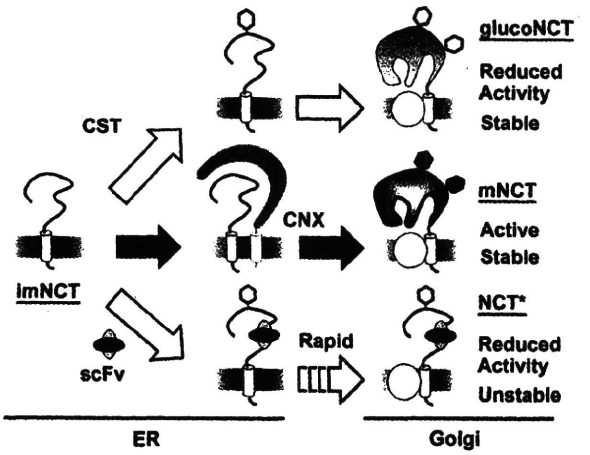

FIGURE 10. **A putative model for the mode of action of 5201F.** In biosynthetic pathway of the γ-secretase (*black arrows*), folding and glycosylation states of NCT are monitored by CNX in the ER. After the assembly of the γ-secretase complex together with PS, APH-1, and PEN-2 (*white circle*), NCT ECD is glycosylated with complex oligosaccharides (*black hexagon*) in the Golgi. CST treatment yields the stable γ-secretase complex containing NCT with aberrant glycosylation (*white hexagon*), which reduces the proteolytic activity. 5201F binding to NCT ECD inhibits the functional folding and glucose trimming to form the unstable and inactive γ-secretase complex with NCT*. *mNCT* and *imNCT* represent mature and immature NCT, respectively.

Endo H-resistant glycosylation of NCT, suggesting that the quality control and the trafficking system for the prefunctional γ-secretase in the ER are altered upon 5201F expression. In general, the folding and maturation states of glycoproteins are monitored by the CNX cycle. Properly folded glycoproteins escape this cycle and are sorted out from the ER. Trypsin resistance of NCT is tightly correlated with the proteolytic activity of the γ-secretase complex and may reflect its structural change in the ER (17), whereas the molecular basis of this conformational change has not been clarified to date. Of note, NCT fused with ER retention dilysine signal at the C terminus retained the ability to form the functional γ-secretase complex and is sorted out to the cell surface (49, 50). In addition, after trypsin digestion, the immunoreactivity of the C terminus of mature NCT was preserved, and no molecular weight change was observed (17). These results suggest that the most C terminus of NCT is also tightly folded in the functional γ-secretase complex. Thus, the folding state of NCT throughout the molecule might be under surveillance by ER-associated chaperones (*i.e.* CNX) and/or trafficking-related molecules (*e.g.* Rer1, coatmer subunits) as a molecular signature for the functional assembly of the γ-secretase complex. Incorporation of 5201F would interrupt the functional folding of NCT and the binding with CNX; the latter presumably caused the aberrant escape of the γ-secretase complex from the CNX cycle, thereby leading to the destabilization of the γ-secretase complex.

An ineffective CNX cycle is also caused by the inhibition of glucose trimming. The treatment with CST induced the accumulation of the glucosylated NCT polypeptides and reduced the γ-secretase activity. In general, aberrant glucosylated proteins generated by CST treatment are rapidly transported out from the ER or degraded by ER-associated degradation (46, 54, 55). However, our results showed that biochemical characteristics of the γ-secretase were unaffected by CST, whereas the intrinsic proteolytic activity was reduced. In contrast, it has been shown that treatment by kifunensine, which inhibits the mannose trimming occurring at the later stage of glycosyl maturation, has no effect on the γ-secretase activity (16, 17), suggesting that the glucose/mannose trimming was dispensable for the proper folding of NCT and the formation of the γ-secretase complex. Rather, our data indicate that the glucosyl state of NCT *per se* is involved in the specific enzymatic activity, suggesting the functional significance of the CNX cycle in the biogenesis of the γ-secretase complex. The analysis of 648/ATAA mutant NCT also supported our notion that the conformational maturation of NCT determines the amount, but not the intrinsic activity, of the functional γ-secretase complex. Although the molecular mechanism(s) by which the glycosylation of NCT modulates the intramembrane cleavage remain unknown, aberrant glucosylated NCT might have lesser activity in the substrate-capturing function.

We propose a model for the mode of action of 5201F as depicted in Fig. 10. NCT would be an essential component in the γ-secretase complex with dual functions, which were disrupted by the binding with 5201F. The properly glycosylated and folded NCT might function not only as a substrate receptor (19) but as a gatekeeper for the trafficking and the stability of the γ-secretase complex (20). Our data presented here also expand the repertoire of antibody-based functional reagents valuable for the cell biology research on the γ-secretase. To modify/engineer their binding profile, scFvs can be applicable to phage display, to which "rational design and directed molecular evolution" process with high throughput platform is applicable (56). In addition, structural studies using scFv have provided crucial information for the rational development of the small compound targeting protein-protein interactions (57).

Notably, amino acid substitutions at certain sites in NCT ECD differently affected the Aβ generation and Notch processing (20). Thus, search for small compounds or peptides targeting NCT ECD might provide a new class of biological tools as well as therapeutics for γ-secretase modulation. Further investigations including structural analyses of NCT ECD complexed with scFvs would shed light on the molecular mechanism of the functional assembly of γ-secretase and the role of NCT ECD in the γ-secretase-mediated intramembrane cleavage.

Acknowledgments—We acknowledge Drs. Keiro Shirotani (Fukushima Medical University), Harald Steiner, Christian Haass (Ludwig-Maximilians-University), Gopal Thinakaran, Sangram Sisodia (The University of Chicago), Haruhiko Fuwa (Tohoku University), Satoshi Yokoshima, and Tohru Fukuyama (The University of Tokyo) for valuable reagents. We are also grateful to our current/previous laboratory members for helpful discussions and technical assistance.

REFERENCES

1. Tomita, T. (2009) *Expert Rev. Neurother.* **9,** 661–679
2. Wolfe, M. S. (2009) *Semin. Cell Dev. Biol.* **20,** 219–224
3. Takasugi, N., Tomita, T., Hayashi, I., Tsuruoka, M., Niimura, M., Takahashi, Y., Thinakaran, G., and Iwatsubo, T. (2003) *Nature* **422,** 438–441
4. Selkoe, D. J., and Wolfe, M. S. (2007) *Cell* **131,** 215–221
5. Spasic, D., and Annaert, W. (2008) *J. Cell Sci.* **121,** 413–420
6. Sato, C., Morohashi, Y., Tomita, T., and Iwatsubo, T. (2006) *J. Neurosci* **26,** 12081–12088
7. Tolia, A., Chávez-Gutiérrez, L., and De Strooper, B. (2006) *J. Biol. Chem.* **281,** 27633–27642
8. Niimura, M., Isoo, N., Takasugi, N., Tsuruoka, M., Ui-Tei, K., Saigo, K., Morohashi, Y., Tomita, T., and Iwatsubo, T. (2005) *J. Biol. Chem.* **280,** 12967–12975
9. Isoo, N., Sato, C., Miyashita, H., Shinohara, M., Takasugi, N., Morohashi, Y., Tsuji, S., Tomita, T., and Iwatsubo, T. (2007) *J. Biol. Chem.* **282,** 12388–12396
10. Yu, G., Nishimura, M., Arawaka, S., Levitan, D., Zhang, L., Tandon, A., Song, Y. Q., Rogaeva, E., Chen, F., Kawarai, T., Supala, A., Levesque, L., Yu, H., Yang, D. S., Holmes, E., Milman, P., Liang, Y., Zhang, D. M., Xu, D. H., Sato, C., Rogaev, E., Smith, M., Janus, C., Zhang, Y., Aebersold, R., Farrer, L. S., Sorbi, S., Bruni, A., Fraser, P., and St George-Hyslop, P. (2000) *Nature* **407,** 48–54
11. Leem, J. Y., Vijayan, S., Han, P., Cai, D., Machura, M., Lopes, K. O., Veselits, M. L., Xu, H., and Thinakaran, G. (2002) *J. Biol. Chem.* **277,** 19236–19240
12. Kaether, C., Lammich, S., Edbauer, D., Ertl, M., Rietdorf, J., Capell, A., Steiner, H., and Haass, C. (2002) *J. Cell Biol.* **158,** 551–561
13. Kimberly, W. T., LaVoie, M. J., Ostaszewski, B. L., Ye, W., Wolfe, M. S., and Selkoe, D. J. (2002) *J. Biol. Chem.* **277,** 35113–35117
14. Tomita, T., Katayama, R., Takikawa, R., and Iwatsubo, T. (2002) *FEBS Lett.* **520,** 117–121
15. Yang, D. S., Tandon, A., Chen, F., Yu, G., Yu, H., Arawaka, S., Hasegawa, H., Duthie, M., Schmidt, S. D., Ramabhadran, T. V., Nixon, R. A., Mathews, P. M., Gandy, S. E., Mount, H. T., St George-Hyslop, P., and Fraser, P. E. (2002) *J. Biol. Chem.* **277,** 28135–28142
16. Herreman, A., Van Gassen, G., Bentahir, M., Nyabi, O., Craessaerts, K., Mueller, U., Annaert, W., and De Strooper, B. (2003) *J. Cell Sci.* **116,** 1127–1136
17. Shirotani, K., Edbauer, D., Capell, A., Schmitz, J., Steiner, H., and Haass, C. (2003) *J. Biol. Chem.* **278,** 16474–16477
18. Fagan, R., Swindells, M., Overington, J., and Weir, M. (2001) *Trends Biochem. Sci.* **26,** 213–214
19. Shah, S., Lee, S. F., Tabuchi, K., Hao, Y. H., Yu, C., LaPlant, Q., Ball, H., Dann, C. E., 3rd, Südhof, T., and Yu, G. (2005) *Cell* **122,** 435–447
20. Chávez-Gutiérrez, L., Tolia, A., Maes, E., Li, T., Wong, P. C., and de Strooper, B. (2008) *J. Biol. Chem.* **283,** 20096–20105
21. Holliger, P., and Hudson, P. J. (2005) *Nat. Biotechnol.* **23,** 1126–1136
22. Miller, T. W., and Messer, A. (2005) *Mol. Ther.* **12,** 394–401
23. Stocks, M. (2005) *Curr. Opin. Chem. Biol.* **9,** 359–365
24. Verbeke, K., Gils, A., and Declerck, P. J. (2004) *J. Thromb. Haemost.* **2,** 298–305
25. Arbel, M., Yacoby, I., and Solomon, B. (2005) *Proc. Natl. Acad. Sci. U.S.A.* **102,** 7718–7723
26. Gal-Tanamy, M., Zemel, R., Berdichevsky, Y., Bachmatov, L., Tur-Kaspa, R., and Benhar, I. (2005) *J. Mol. Biol.* **347,** 991–1003
27. Paganetti, P., Calanca, V., Galli, C., Stefani, M., and Molinari, M. (2005) *J. Cell Biol.* **168,** 863–868
28. Farady, C. J., Sun, J., Darragh, M. R., Miller, S. M., and Craik, C. S. (2007) *J. Mol. Biol.* **369,** 1041–1051
29. Mikkelsen, J. H., Gyrup, C., Kristensen, P., Overgaard, M. T., Poulsen, C. B., Laursen, L. S., and Oxvig, C. (2008) *J. Biol. Chem.* **283,** 16772–16780
30. Hayashi, I., Urano, Y., Fukuda, R., Isoo, N., Kodama, T., Hamakubo, T., Tomita, T., and Iwatsubo, T. (2004) *J. Biol. Chem.* **279,** 38040–38046
31. Ogura, T., Mio, K., Hayashi, I., Miyashita, H., Fukuda, R., Kopan, R., Kodama, T., Hamakubo, T., Iwatsubo, T., Tomita, T., and Sato, C. (2006) *Biochem. Biophys. Res. Commun.* **343,** 525–534
32. Li, T., Ma, G., Cai, H., Price, D. L., and Wong, P. C. (2003) *J. Neurosci.* **23,** 3272–3277
33. Watanabe, N., Tomita, T., Sato, C., Kitamura, T., Morohashi, Y., and Iwatsubo, T. (2005) *J. Biol. Chem.* **280,** 41967–41975
34. Tomita, T., Takikawa, R., Koyama, A., Morohashi, Y., Takasugi, N., Saido, T. C., Maruyama, K., and Iwatsubo, T. (1999) *J. Neurosci.* **19,** 10627–10634
35. Tomita, T., Watabiki, T., Takikawa, R., Morohashi, Y., Takasugi, N., Kopan, R., De Strooper, B., and Iwatsubo, T. (2001) *J. Biol. Chem.* **276,** 33273–33281
36. Tomita, T., Maruyama, K., Saido, T. C., Kume, H., Shinozaki, K., Tokuhiro, S., Capell, A., Walter, J., Grünberg, J., Haass, C., Iwatsubo, T., and Obata, K. (1997) *Proc. Natl. Acad. Sci. U.S.A.* **94,** 2025–2030
37. Morohashi, Y., Kan, T., Tominari, Y., Fuwa, H., Okamura, Y., Watanabe, N., Sato, C., Natsugari, H., Fukuyama, T., Iwatsubo, T., and Tomita, T. (2006) *J. Biol. Chem.* **281,** 14670–14676
38. Takahashi, Y., Hayashi, I., Tominari, Y., Rikimaru, K., Morohashi, Y., Kan, T., Natsugari, H., Fukuyama, T., Tomita, T., and Iwatsubo, T. (2003) *J. Biol. Chem.* **278,** 18664–18670
39. Fuwa, H., Takahashi, Y., Konno, Y., Watanabe, N., Miyashita, H., Sasaki, M., Natsugari, H., Kan, T., Fukuyama, T., Tomita, T., and Iwatsubo, T. (2007) *ACS Chem. Biol.* **2,** 408–418
40. Saitoh, R., Ohtomo, T., Yamada, Y., Kamada, N., Nezu, J., Kimura, N., Funahashi, S., Furugaki, K., Yoshino, T., Kawase, Y., Kato, A., Ueda, O., Jishage, K., Suzuki, M., Fukuda, R., Arai, M., Iwanari, H., Takahashi, K., Sakihama, T., Ohizumi, I., Kodama, T., Tsuchiya, M., and Hamakubo, T. (2007) *J. Immunol. Methods* **322,** 104–117
41. Walker, E. S., Martinez, M., Wang, J., and Goate, A. (2006) *J. Neurochem.* **98,** 300–309
42. Ratovitski, T., Slunt, H. H., Thinakaran, G., Price, D. L., Sisodia, S. S., and Borchelt, D. R. (1997) *J. Biol. Chem.* **272,** 24536–24541
43. Kato, K., and Kamiya, Y. (2007) *Glycobiology* **17,** 1031–1044
44. Caramelo, J. J., and Parodi, A. J. (2008) *J. Biol. Chem.* **283,** 10221–10225
45. Morais, V. A., Brito, C., Pijak, D. S., Crystal, A. S., Fortna, R. R., Li, T., Wong, P. C., Doms, R. W., and Costa, J. (2006) *Biochim Biophys Acta* **1762,** 802–810
46. Saul, R., Chambers, J. P., Molyneux, R. J., and Elbein, A. D. (1983) *Arch. Biochem. Biophys.* **221,** 593–597
47. Hammond, C., Braakman, I., and Helenius, A. (1994) *Proc. Natl. Acad. Sci. U.S.A.* **91,** 913–917
48. LaVoie, M. J., Fraering, P. C., Ostaszewski, B. L., Ye, W., Kimberly, W. T., Wolfe, M. S., and Selkoe, D. J. (2003) *J. Biol. Chem.* **278,** 37213–37222
49. Capell, A., Beher, D., Prokop, S., Steiner, H., Kaether, C., Shearman, M. S., and Haass, C. (2005) *J. Biol. Chem.* **280,** 6471–6478
50. Kim, S. H., Yin, Y. I., Li, Y. M., and Sisodia, S. S. (2004) *J. Biol. Chem.* **279,** 48615–48619
51. Kaether, C., Scheuermann, J., Fassler, M., Zilow, S., Shirotani, K., Valkova, C., Novak, B., Kacmar, S., Steiner, H., and Haass, C. (2007) *EMBO Rep.* **8,**

743–748
52. Kim, J., Kleizen, B., Choy, R., Thinakaran, G., Sisodia, S. S., and Schekman, R. W. (2007) *J. Cell Biol.* **179,** 951–963
53. Spasic, D., Raemaekers, T., Dillen, K., Declerck, I., Baert, V., Serneels, L., Füllekrug, J., and Annaert, W. (2007) *J. Cell Biol.* **176,** 629–640
54. Keller, S. H., Lindstrom, J., and Taylor, P. (1998) *J. Biol. Chem.* **273,** 17064–17072
55. Marcus, N. Y., and Perlmutter, D. H. (2000) *J. Biol. Chem.* **275,** 1987–1992
56. Sidhu, S. S., and Koide, S. (2007) *Curr. Opin. Struct. Biol.* **17,** 481–487
57. Novoa de Armas, H., Dewilde, M., Verbeke, K., De Maeyer, M., and Declerck, P. J. (2007) *Structure* **15,** 1105–1116

THE JOURNAL OF BIOLOGICAL CHEMISTRY VOL. 284, NO. 3, pp. 1373–1384, January 16, 2009

S-Palmitoylation of γ-Secretase Subunits Nicastrin and APH-1*[S]

Received for publication, August 18, 2008, and in revised form, November 20, 2008 Published, JBC Papers in Press, November 20, 2008, DOI 10.1074/jbc.M806380200

Haipeng Cheng[‡], Kulandaivelu S. Vetrivel[‡], Renaldo C. Drisdel[‡], Xavier Meckler[‡], Ping Gong[‡], Jae Yoon Leem[‡], Tong Li[§], Meghan Carter[‡], Ying Chen[‡], Phuong Nguyen[¶], Takeshi Iwatsubo[‖], Taisuke Tomita[‖**], Philip C. Wong[§], William N. Green[‡], Maria Z. Kounnas[¶], and Gopal Thinakaran[‡ ‡‡§§1]**

*From the Departments of [‡]Neurobiology, [‡‡]Neurology, and [§§]Pathology, The University of Chicago, Chicago, Illinois 60637, the [§]Department of Pathology, The Johns Hopkins University School of Medicine, Baltimore, Maryland 21205, [¶]TorreyPines Therapeutics, Inc., La Jolla, California 92037, the [‖]Department of Neuropathology and Neuroscience, Graduate School of Pharmaceutical Sciences, The University of Tokyo, Hongo 7-3-1, Bunkyo, Tokyo 113-0033, Japan, and the **Core Research for Evolutional Science and Technology, Japan Science and Technology Corporation, Hongo 7-3-1, Bunkyo, Tokyo 113-0033, Japan*

Proteolytic processing of amyloid precursor protein (APP) by β- and γ-secretases generates β-amyloid (Aβ) peptides, which accumulate in the brains of individuals affected by Alzheimer disease. Detergent-resistant membrane microdomains (DRM) rich in cholesterol and sphingolipid, termed lipid rafts, have been implicated in Aβ production. Previously, we and others reported that the four integral subunits of the γ-secretase associate with DRM. In this study we investigated the mechanisms underlying DRM association of γ-secretase subunits. We report that in cultured cells and in brain the γ-secretase subunits nicastrin and APH-1 undergo *S*-palmitoylation, the post-translational covalent attachment of the long chain fatty acid palmitate common in lipid raft-associated proteins. By mutagenesis we show that nicastrin is *S*-palmitoylated at Cys[689], and APH-1 is *S*-palmitoylated at Cys[182] and Cys[245]. *S*-Palmitoylation-defective nicastrin and APH-1 form stable γ-secretase complexes when expressed in knock-out fibroblasts lacking wild type subunits, suggesting that *S*-palmitoylation is not essential for γ-secretase assembly. Nevertheless, fractionation studies show that *S*-palmitoylation contributes to DRM association of nicastrin and APH-1. Moreover, pulse-chase analyses reveal that *S*-palmitoylation is important for nascent polypeptide stability of both proteins. Co-expression of *S*-palmitoylation-deficient nicastrin and APH-1 in cultured cells neither affects Aβ40, Aβ42, and AICD production, nor intramembrane processing of Notch and N-cadherin. Our findings suggest that *S*-palmitoylation plays a role in stability and raft localization of nicastrin and APH-1, but does not directly modulate γ-secretase processing of APP and other substrates.

Alzheimer disease is the most common among neurodegenerative diseases that cause dementia. This debilitating disorder is pathologically characterized by the cerebral deposition of 39–42 amino acid peptides termed Aβ, which are generated by proteolytic processing of amyloid precursor protein (APP)[2] by β- and γ-secretases (1, 2). The β-site APP cleavage enzyme 1 cleaves full-length APP within its luminal domain to generate a secreted ectodomain leaving behind a C-terminal fragment (β-CTF). γ-Secretase cleaves β-CTF within the transmembrane domain to release Aβ and APP intracellular C-terminal domain (AICD). γ-Secretase is a multiprotein complex, comprising at least four subunits: presenilins (PS1 and PS2), nicastrin, APH-1, and PEN-2 for its activity (3). PS1 is synthesized as a 42–43-kDa polypeptide and undergoes highly regulated endoproteolytic processing within the large cytoplasmic loop domain connecting putative transmembrane segments 6 and 7 to generate stable N-terminal (NTF) and C-terminal fragments (CTF) by an uncharacterized proteolytic activity (4). This endoproteolytic event has been identified as the activation step in the process of PS1 maturation as it assembles with other γ-secretase subunits (3). Nicastrin is a heavily glycosylated type I membrane protein with a large ectodomain that has been proposed to function in substrate recognition and binding (5), but this putative function has not been confirmed by others (6). APH-1 is a seven-transmembrane protein encoded by two human or three rodent genes that are alternatively spliced (7). Although PS1 (or PS2), nicastrin, APH-1, and PEN-2 are sufficient for γ-secretase processing of APP, a type I membrane protein, termed p23 (also referred toTMP21), was recently identified as a γ-secretase component that modulates γ-secretase activity and regulates secretory trafficking of APP (8, 9).

A growing number of type I integral membrane proteins has been identified as γ-secretase substrates within the last few years, including Notch1 homologues, Notch ligands, Delta and

* This work was supported, in whole or in part, by National Institutes of Health Grants AG021495 (to G. T.), AG019070 (to G. T.), NS45150 (to P. C. W.), and P01 NS047308 (to P. C. W.). This work was also supported by grants from the Alzheimer Association (to G. T. and K. S. V.) and American Health Assistance Foundation (to G. T.). The costs of publication of this article were defrayed in part by the payment of page charges. This article must therefore be hereby marked "*advertisement*" in accordance with 18 U.S.C. Section 1734 solely to indicate this fact.

[S] The on-line version of this article (available at http://www.jbc.org) contains supplemental Figs. S1–S7.

[1] To whom correspondence should be addressed: Dept. of Neurobiology, The University of Chicago, Knapp R212, 924 E. 57th St., Chicago, IL 60637. Tel.: 773-834-3752; Fax: 773-834-3808; E-mail: gopal@uchicago.edu.

[2] The abbreviations used are: APP, amyloid precursor protein; Aβ, β-amyloid; AICD, APP intracellular domain; BFA, brefeldin A; CTF, C-terminal fragment; MEF, mouse embryonic fibroblasts; NICD, Notch intracellular domain; PS, presenilin(s); NTF, N-terminal fragment; WT, wild-type; DRM, detergent-resistant membrane; HEK, human embryonic kidney; biotin-BMCC, 1-biotinamido-4-(4′-[maleimidoethyl-cyclohexane]-carboxamido)butane; ELISA, enzyme-linked immunosorbent assay; CHX, cycloheximide; ER, endoplasmic reticulum; mAb, monoclonal antibody; CHAPSO, 3-[(3-cholamidopropyl)dimethylammonio]-2-hydroxy-1-propanesulfonic acid.

Jagged, cell adhesion receptors N- and E-cadherins, low density lipoprotein receptor-related protein, ErbB-4, netrin receptor DCC, and others (10). Mounting evidence suggests that APP processing occurs within cholesterol- and sphingolipid-enriched lipid rafts, which are biochemically defined as detergent-resistant membrane microdomains (DRM) (11, 12). Previously we reported that each of the γ-secretase subunits localizes in lipid rafts in post-Golgi and endosome membranes enriched in syntaxin 6 (13). Moreover, loss of γ-secretase activity by gene deletion or exposure to γ-secretase inhibitors results in the accumulation of APP CTFs in lipid rafts indicating that cleavage of APP CTFs likely occurs in raft microdomains (14). In contrast, CTFs derived from Notch1, Jagged2, N-cadherin, and DCC are processed by γ-secretase in non-raft membranes (14). The mechanisms underlying association of γ-secretase subunits with lipid rafts need further clarification to elucidate spatial segregation of amyloidogenic processing of APP in membrane microdomains.

Post-translational *S*-palmitoylation is increasingly recognized as a potential mechanism for regulating raft association, stability, intracellular trafficking, and function of several cytosolic and transmembrane proteins (15–17). *S*-palmitoylation refers to the addition of 16-carbon palmitoyl moiety to certain cysteine residues through thioester linkage. Cysteines close to transmembrane domains or membrane-associated domains in non-integral membrane proteins are preferred *S*-palmitoylation sites, although no conserved motif has been identified (18). Palmitoylation modifies numerous neuronal proteins, including postsynaptic density protein PSD-95 (19), a-amino-3-hydroxyl-5-methyl-4-isoxazole propionic acid receptors (20), nicotinic α7 receptors (21), neuronal t-SNAREs SNAP-25, synaptobrevin 2 and synaptogagmin (22, 23), neuronal growth-associated protein GAP-43 (24), protein kinase CLICK-III (CL3)/CaMKIγ (25), β-secretase (26), and Huntingtin (27). Although palmitoylation can occur *in vitro* without the involvement of an enzyme, a family of palmitoyltransferases that specifically catalyze *S*-palmitoylation has been identified (28, 29).

In this study, we have identified *S*-palmitoylation of γ-secretase subunits nicastrin and APH-1, and characterized its role on DRM association, protein stability, and γ-secretase enzyme activities. We show that nicastrin is *S*-palmitoylated at Cys^{689}, and APH-1 at Cys^{182} and Cys^{245}. Mutagenesis of palmitoylation sites results in increased degradation of nascent nicastrin and APH-1 polypeptides and reduced association with DRM. Nevertheless, in cultured cells overexpression of *S*-palmitoylation-deficient nicastrin and APH-1 does not modulate γ-secretase processing of APP or other substrates.

EXPERIMENTAL PROCEDURES

Plasmids—cDNAs encoding nicastrin mutant C689S, and APH-1 mutants C182S, C245S, and C182S/C245S were generated by overlap PCR, and all PCR products were verified by sequencing. Expression plasmids containing PS1, nicastrin, APH-1aL-Myc-His, and PEN-2 were used for transient transfection studies. The cDNAs encoding nicastrin, APH-1aL-6Myc-His, and PEN-2 were subcloned into retroviral expression vectors pLHCX, pMXs-puro (30), and pMXs-blasticidin, respectively, and used for the generation of stably transduced pools. APP695Swe, NotchΔEMV-6Myc (31), and APP C99-6Myc (32) were subcloned into pMXs retrovirus vector and used for transient infection. The plasmid encoding His-Myc-tagged ubiquitin was provided by Dr. Ron Kopito (Stanford University) (33).

Cell Culture—$NCT^{-/-}$ and $APH\text{-}1ac^{-/-}$ mouse embryonic fibroblasts (MEF),[3] and HEK293 were cultured in Dulbecco's modified Eagle's medium (Invitrogen) supplemented with 10% fetal bovine serum. Mouse N2a neuroblastoma cell lines were maintained in the medium above mixed with 1:1 Opti-MEM (Invitrogen). $PS1^{-/-}/PS2^{-/-}$ embryonic stem cells were cultured in embryonic stem cell medium supplemented with leukemia inhibitory factor (34). HEK293-based Plat-E packaging cells were transfected with cDNAs cloned in retroviral vectors. 48 h after transfection, media were collected and clarified by centrifugation at 800 × *g* for 5 min. Target cells were infected by adding virus-containing supernatant in the presence of 4 μg/ml of Polybrene. Stable MEF pools were generated by infection of $NCT^{-/-}$ and $APH\text{-}1ac^{-/-}$ MEF with retroviruses encoding nicastrin or APH-1aL, respectively. $NCT^{-/-}$dWt and dMut pools were generated by sequential infection of $NCT^{-/-}$ MEF with retroviruses encoding WT nicastrin and APH-1 (dWt) or nicastrin C689S and APH-1aL C182S/C245S (dMut), respectively. Similarly, N2aSwe dWt and dMut pools were generated by sequential infection of N2a cell line Swe10, which expresses human APP695 harboring the "Swedish" double mutants (35). Stably transduced cells were selected as pools in 5 μg/ml puromycin and/or 400 μg/ml hygromycin. N2a cells overexpressing PS1 and APPSwe were infected with PEN-2 retrovirus and N2aPAP cells were selected as a pool in 5 μg/ml blasticidin. N2aPAP dWt and dMut were generated by sequential transduction with nicastrin and APH-1aL retroviruses as described above.

Antibodies—The following antibodies were used in this study: $PS1_{NT}$ and α PS1Loop were raised against residues 1–65 and 263–407 of PS1, respectively (4, 36); SP716 was raised against residues 62–93 of nicastrin (37); PNT2 was raised against residues 1–26 of PEN-2 (13). Rabbit polyclonal antibody CTM1 was raised against a synthetic peptide corresponding to the C-terminal 15 amino acids of APP followed by the c-Myc epitope (MEQKLISEEDLN). Rabbit polyclonal antibody A1tag was raised against a synthetic peptide corresponding to the C-terminal 15 amino acids of APH-1aL followed by residues SSRGPSSAEVLLLPVS. This antibody reacts with mouse and human APH-1. Polyclonal APH-1aL antibody O2C2 was a gift of Drs. Paul Fraser and Peter St. George-Hyslop (The University of Toronto). Monoclonal antibody A5226 (38) specifically reacts with human nicastrin.[4] The following antibodies were purchased from commercial sources: flotillin-2 and N-cadherin from BD Transduction Laboratories, 9E10 from ATCC, and 4G8 from Covance.

S-Palmitoylation Assays—Labeling of *S*-palmitoylated residues was carried out as described previously with some modifications (39). Briefly, transfected HEK293 cells were lysed in 1 ml of lysis buffer (150 mM NaCl, 5 mM EDTA, 50 mM Tris-HCl,

[3] T. Li and P. C. Wong, manuscript in preparation.
[4] I. Hayashi, S. Takatori, T. Iwatsubo, and T. Tomita, unpublished results.

pH 7.4, 1% Triton X-100, protease inhibitor mixture (Sigma), and 50 mM *N*-ethylmaleimide). Aliquots of lysates were incubated with specific antibodies to immunoprecipitate each γ-secretase subunit. Immunoprecipitated proteins bound to agarose beads were treated with 1 M hydroxylamine (pH 7.4) at room temperature to cleave the thioester bond and expose a reactive cysteine by detaching the palmitic acid. Subsequently, the beads were incubated with 0.2 μM 1-biotinamido-4-(4'-[maleimidoethyl-cyclohexane]-carboxamido)butane (biotin-BMCC) (pH 6.2) at 4 °C for 2 h to label reactive cysteine residues. Following SDS-PAGE and transfer to polyvinylidene difluoride membranes, the blots were reacted with streptavidin-horseradish peroxidase to detect biotin-BMCC-labeled proteins. For biotin-BMCC labeling of nicastrin, cells were lysed in methylthiolation buffer (20 mM Tris-HCl, pH 7.7, 2.5% SDS, 20 mM *S*-methylmethanethiosulfonic acid, 1 mM EDTA, and 0.1 mM neocuproine). After incubation at 50 °C for 30 min, proteins were precipitated from free *S*-methylmethanethiosulfonic acid by the addition of 2 volumes of cold acetone and centrifuged. The pellets were resuspended in lysis buffer containing 1% SDS, and neutralized by adding Triton X-100 to a final concentration of 5% before immunoprecipitating nicastrin. For acyl-biotin exchange labeling of subunits expressed in brain, the nicastrin and APH-1 were immunoprecipitated from 1-month-old mouse brain homogenates using antibodies SP716 and O2C2, respectively. For [^{3}H]palmitic acid labeling, transfected HEK293 cells were starved for 30 min in Dulbecco's modified Eagle's medium containing 1% dialyzed fetal bovine serum and incubated with 100 μCi/ml of [10, 11-^{3}H]palmitic acid (American Radiolabeled Chemicals) for 6 h. Proteins were immunoprecipitated from detergent lysates, fractionated by SDS-PAGE, and detected by phosphorimage analysis.

Metabolic Labeling, Immunoprecipitation, and ELISA—Cells were starved in methionine/cysteine (Met/Cys)-free medium for 30 min and then labeled with 125 μCi/ml of [^{35}S]Met/Cys (MP Biomedicals) for 15 min or 3 h. For pulse-chase studies, cells were labeled for 15 or 30 min and then chased in medium supplemented with 2 mM each of methionine and cysteine, and 30 μg/ml of cycloheximide (CHX) for the indicated periods. Cells were then washed and lysed in IP buffer (50 mM Tris-HCl, pH 7.4, 150 mM NaCl, 0.5% sodium dexoycholate, 0.5% Nonidet P-40, 0.25% SDS, 5 mM EDTA, 0.25 mM phenylmethylsulfonyl fluoride, and a protease inhibitor mixture). [^{35}S]Met/Cys incorporation was measured by trichloroacetic acid precipitation of the lysates and equal amounts of labeled proteins were used for immunoprecipitation analysis. Polyclonal antibody CTM1 was used to precipitate APP and APP CTFs. 4G8 was used to immunoprecipitate Aβ and p3 from the conditioned media. SP716 were used to immunoprecipitate nicastrin. 9E10 was used to immunoprecipitate Myc_6-tagged APH-1aL, NotchΔEMV, and APP C99. Immunoprecipitates were separated by SDS-PAGE, analyzed by phosphorimaging, and quantified using ImageQuant. For ELISA analysis of secreted Aβ, fibroblasts were infected with APPSwe retrovirus for 24 h, and conditioned media were collected 24 h following the addition of fresh culture medium. Conditioned medium from N2aSwe cells were collected following 24 h incubation. The levels of Aβ40 and Aβ42 were quantified using sandwich ELISAs as described previously (9).

AICD Generation Assay—In vitro AICD generation was assayed as described previously (40). $NCT^{-/-}$ cells overexpressing WT or mutant nicastrin and APH-1 in 60-mm dishes were infected with retrovirus encoding APPSwe and harvested 48 h later in buffer A (50 mM HEPES, 150 mM NaCl, 5 mM 1,10-phenanthroline monohydrate, pH 7.4). Cells were homogenized by passing 10 times through a 25-gauge needle and the homogenate was centrifuged at 10,000 × *g* for 15 min. The pellet containing membrane fraction (P10) was resuspended in 500 μl of buffer A. Aliquots of P10 fraction (normalized to protein content) were centrifuged again and resuspended in 30 μl of buffer A supplemented with protease inhibitor mixture (Sigma). The samples were incubated for 2 h on ice (as negative control), or at 37 °C to induce the release of AICD. Then the samples were centrifuged at 10,000 × *g* for 15 min and the supernatant containing soluble proteins was collected and analyzed by Western blotting.

RESULTS

Nicastrin and APH-1 Are S-Palmitoylated—In our search for potential post-translational modifications that might regulate γ-secretase residence in cholesterol-rich membrane microdomains, we turned our attention to the protein *S*-palmitoylation of γ-secretase subunits. The thioester bond linking 16-carbon saturated fatty acid palmitate to cysteine residues of *S*-palmitoylated proteins can be cleaved by hydroxylamine, leaving a free sulfhydryl group, which can be subsequently labeled using a variety of reagents including [^{3}H]*N*-ethylmaleimide and biotin-BMCC (39). Using this *S*-palmitoylation-specific acyl-biotin exchange strategy, we show that two of the four γ-secretase subunits, nicastrin and APH-1, can be specifically modified by biotin-BMCC (Fig. 1*A*). Labeling was successful only when the immunoprecipitates were pretreated with hydroxylamine, which demonstrates that these two subunits undergo *S*-palmitoylation. More importantly, endogenous nicastrin and APH-1 immunoprecipitated from mouse brain can be labeled, indicating that endogenous nicastrin and APH-1 are *S*-palmitoylated in the brain (Fig. 1*B*).

We performed site-directed mutagenesis of cytosolic and transmembrane cysteine residues to identify the sites of *S*-palmitoylation. Nicastrin undergoes *S*-palmitoylation at a single site, Cys^{689} (Fig. 1, *C* and *D*). *In vitro* biotin-BMCC labeling of nicastrin is abolished when Cys^{689} was mutagenized to a serine residue (Fig. 1*C*). Moreover, WT but not C689S mutant nicastrin can be metabolically labeled with [^{3}H]palmitic acid in transfected HEK293 cells (Fig. 1*D*). This *S*-palmitoylation site within the transmembrane domain is conserved in *Caenorhabditis elegans* and vertebrates (Fig. 1*F*). We also identified *S*-palmitoylation at two conserved cysteine residues in APH-1aL (Fig. 1*E*). Mutation of either Cys^{182} or Cys^{245} reduced the extent of labeling with biotin-BMCC, whereas mutation of both Cys^{182} and Cys^{245} completely abolished labeling, identifying these two residues as *S*-palmitoylation sites. These two palmitoylation sites are conserved in all APH-1 isoforms expressed in mouse and human (Fig. 1*F*). We were unable to metabolically label APH-1 using [^{3}H]palmitic acid, likely due to the relatively

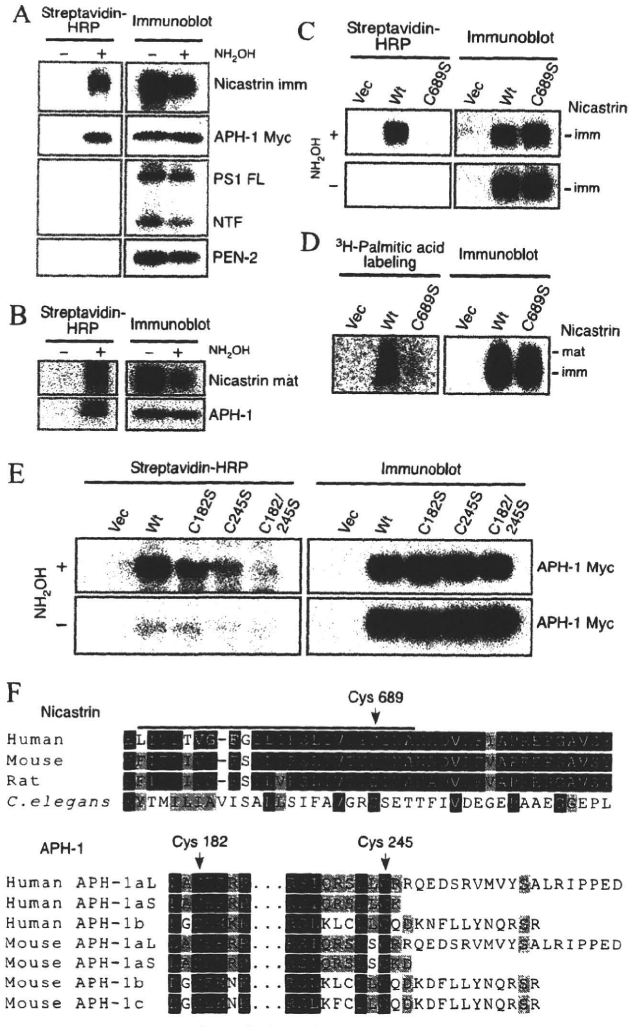

FIGURE 1. **S-Palmitoylation of nicastrin and APH-1.** *A*, acyl-biotin exchange reaction labeling of γ-secretase subunits. Nicastrin, APH-1aL, PS1, or PEN-2 were transiently expressed in HEK293 cells and immunoprecipitated using antibodies SP716, 9E10, $PS1_{NT}$, and PNT2, respectively. Immunoprecipitates were treated or not with hydroxylamine (NH_2OH), followed by incubation with biotin-BMCC to label *S*-palmitoylated cysteine residues. Labeled subunits were visualized by incubating with streptavidin-horseradish peroxidase (*HRP*). The blots were reprobed with specific antibodies to reveal all immunoprecipitated proteins. *B*, acyl-biotin exchange reveals palmitoylation of nicastrin and APH-1 in mouse brain. *C*, mutagenesis identifies Cys^{689} as the only palmitoylated residue in nicastrin. *D*, [^{3}H]palmitic acid labeling of nicastrin. HEK293 cells transiently transfected with WT or C689S nicastrin were metabolically labeled with [^{3}H]palmitic acid for 6 h then immunoprecipitated by SP716 antibody. *E*, mutagenesis identifies that APH-1 undergoes *S*-palmitoylation at Cys^{182} and Cys^{245}. *F*, alignment of the nicastrin and APH-1 sequences near the sites of *S*-palmitoylation was performed using ClustalW2. The transmembrane domain of human nicastrin (amino acids 670–692) is marked by a *horizontal line*.

low rate of palmitoylation of nascent APH-1 or the turnover of palmitate in this subunit. Together, the above results show that two γ-secretase subunits are *S*-palmitoylated *in vitro* and in the brain.

S-Palmitoylation-deficient Nicastrin and APH-1 Assemble γ-Secretase Complex with Other Subunits—The biogenesis, maturation, and stability of each of the γ-secretase components is co-regulated (3). Stable expression of WT or *S*-palmitoylation-deficient nicastrin (C689S) in $NCT^{-/-}$ MEF restored the defects in the accumulation of endoproteolytically derived mature PS1 fragments and PEN-2. Similarly, stable expression of C-terminal tagged WT or *S*-palmitoylation-deficient APH-1aL (C182S/C245S) in $APH1a/c^{-/-}$ MEF (with targeted disruption of mouse *APH1a* and *APH1c* loci) restored the levels of PS1, PEN-2, and nicastrin (Fig. 2*A* and supplemental Fig. S1). We then generated stable $NCT^{-/-}$ MEF pools stably co-expressing WT human nicastrin and WT human APH-1aL (dWt) or *S*-palmitoylation-deficient mutants (dMut). As expected, overexpressed nicastrin and APH-1 undergo *S*-palmitoylation in $NCT^{-/-}$ dWt but not in $NCT^{-/-}$ dMut cells (Fig. 2*B*). Immunoblot analysis revealed that overexpression of *S*-palmitoylation-deficient nicastrin and APH-1 in $NCT^{-/-}$ MEF does not affect endoproteolytic processing of PS1 (Fig. 2*A*), which suggested that *S*-palmitoylation of these subunits is not required for γ-secretase assembly.

We performed co-immunoprecipitation experiments to provide direct evidence for γ-secretase complex formation. Endogenous APH-1 in WT MEF can be readily co-immunoprecipitated by antibodies raised against PS1 NTF or CTF (Fig. 2*C*). Parallel co-immunoprecipitation analysis of $NCT^{-/-}$ dWt and dMut cells revealed that similar levels of Myc-tagged human WT or mutant APH-1 (with retarded mobility on gels compared with endogenous APH-1) and small levels of the remaining mouse APH-1 were complexed with endogenous mouse PS1 in these cells (Fig. 2*C*). Thus, exogenously expressed APH-1 can replace endogenous APH-1 and incorporate into γ-secretase complexes in dWt and dMut pools. Moreover, we found that similar levels of nicastrin, APH-1, PEN-2, and PS1 NTF are co-immunoprecipitated from 1% CHAPSO lysates of dWt and dMut cells using an antibody against PS1 CTF (Fig. 2*D*). We noted that *S*-palmitoylation deficiency results in relative instability of nicastrin and APH-1 (Fig. 3*A*, see below). Therefore, we carried out co-immunoprecipitation of mature γ-secretase complex from cells treated with CHX for 8 h to exclude unstable subunits (41). Comparable levels of nicastrin, APH-1, PS1 NTF, and PEN2 were immunoprecipitated from dWt and dMut cells (Fig. 2*D*). Similar results were obtained when an antibody against PS1 NTF was used for the co-immunoprecipitation (supplemental Fig. S2). Together, these results indicate that *S*-palmitoylation-deficient human nicastrin and APH-1 can assemble with endogenous PS1 and PEN-2 to form γ-secretase complexes.

S-Palmitoylation Contributes to the Stability of Nascent Nicastrin and APH-1—In several independent MEF pools we noted relatively lower steady-state levels of *S*-palmitoylation-deficient nicastrin and APH-1 as compared with WT subunits, raising the possibility that *S*-palmitoylation might regulate the stability of nascent nicastrin and APH-1. Indeed, when $NCT^{-/-}$ cells expressing WT or C689S mutant nicastrin were treated with CHX, we can readily observe the relative instability of palmitoylation-deficient nicastrin (Fig. 3*A*). Similar results were obtained for palmitoylation-deficient APH-1 expressed in $APH1a/c^{-/-}$ MEF (Fig. 3*B*). To confirm these findings, we performed pulse-chase experiments in $NCT^{-/-}$ dWt and $NCT^{-/-}$ dMut cells using [^{35}S]Met/Cys labeling. By pulse labeling, we found that the level of synthesis of nicastrin and APH-1 was very similar in dWt and dMut cells. However, *S*-palmitoylation-

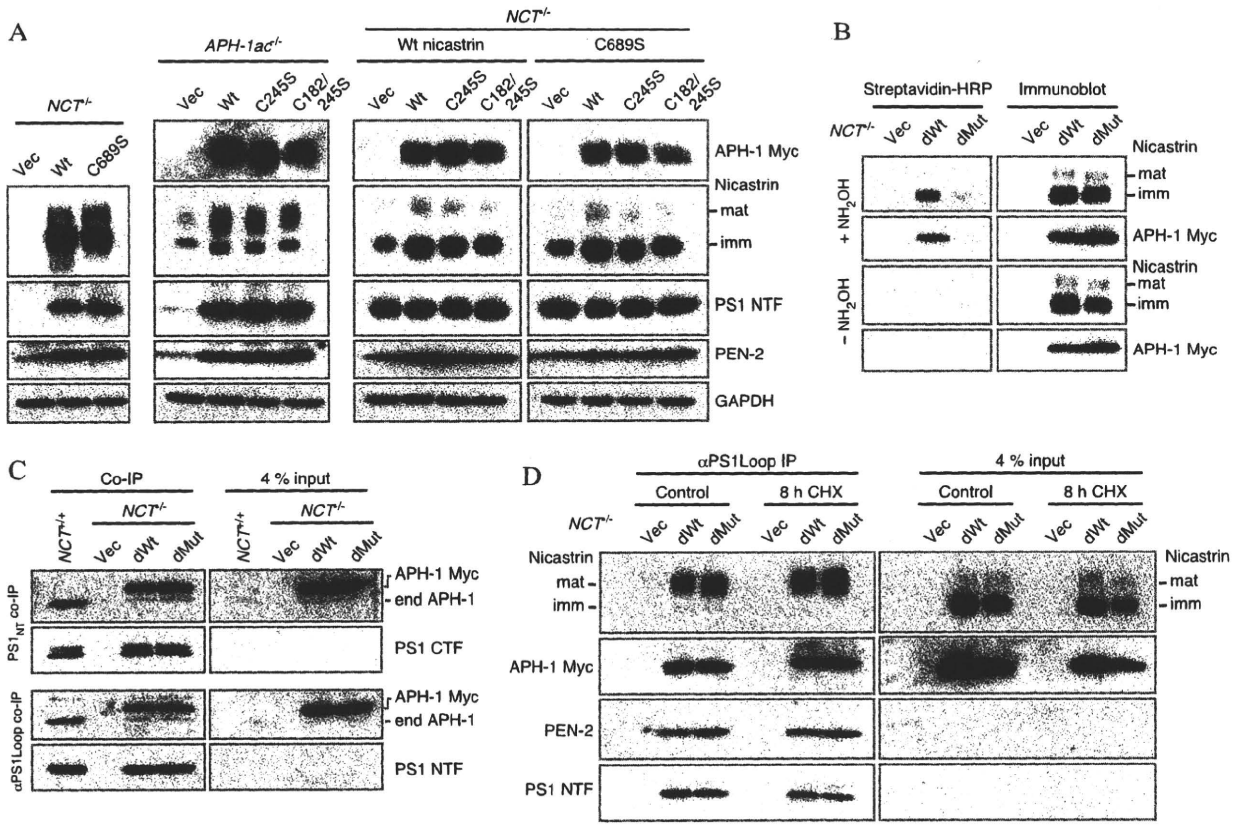

FIGURE 2. **S-Palmitoylation-deficient nicastrin and APH-1 assemble γ-secretase with other subunits.** *A*, immunoblot analysis of γ-secretase subunits in knock-out MEF. WT or Cys mutant nicastrin and APH-1 were stably co-expressed by retroviral transduction in $NCT^{-/-}$ and $APH\text{-}1ac^{-/-}$ MEF, respectively. For control, MEFs were transduced with empty retroviral vector (*Vec*). $NCT^{-/-}$ MEF were also sequentially transduced with nicastrin and APH-1 to generate double WT (*dWt*) and double mutant (*dMut*) pools. Immunoblots were performed to monitor transgene expression, as well as rescue stability and endoproteolytic processing of PS1, maturation of nicastrin, and stabilization of PEN2. *B*, acyl-biotin exchange labeling of nicastrin and APH-1 in $NCT^{-/-}$ dWt and dMut MEF, as described in the legend to Fig. 1. *C*, co-immunoprecipitation analysis of APH-1 replacement. $NCT^{-/-}$ dWt and dMut MEF were lysed in a buffer containing 1% CHAPSO and immunoprecipitated with $PS1_{NT}$ or αPS1Loop antibodies. The blots were sequentially probed with polyclonal APH-1 antibody, A1tag, and $PS1_{NT}$ or αPS1Loop antibodies. *D*, co-immunoprecipitation analysis of PS1 complexes. $NCT^{-/-}$ dWt and dMut MEF were lysed in 1% CHAPSO buffer and PS1 association with nicastrin, APH-1, and PEN-2 were analyzed by co-immunoprecipitation using αPS1Loop antibody, at steady state (control) and 8 h after translation arrest in the presence of cycloheximide (*CHX*). The blots were sequentially probed with antibodies against each γ-secretase subunit (SP716, 9E10, PNT2, and $PS1_{NT}$). Note that the signals for PEN-2 and PS1 CTF are much stronger in PS1 co-immunoprecipitates (*IP*) compared with 4% input lanes, where they are detectible only upon longer exposure of the blots to films (not shown).

deficient nicastrin and APH-1 polypeptides degraded at a significantly faster rate as compared with WT polypeptides (Fig. 3, *C* and *D*). Nevertheless, maturation of nicastrin into a complex glycosylated, slower migrating species was not affected by *S*-palmitoylation deficiency. To formally establish that endogenous immature nicastrin is indeed modified by *S*-palmitoylation, we carried out experiments in embryonic stem cell lines cultured from $PS1^{-/-}/PS2^{-/-}$ embryos. Direct metabolic labeling using [^{3}H]palmitic acid and acyl thiol exchange labeling using [^{3}H]*N*-ethylmaleimide revealed *S*-palmitoylation of immature nicastrin, which is present in $PS1^{-/-}/PS2^{-/-}$ cells (37) (supplemental Fig. S3). These results indicate that excess nascent nicastrin C689S and APH-1 C182S/C245S (that are likely not part of PS1 complex) are unstable as compared with WT subunits overexpressed at similar levels, suggesting one potential function for *S*-palmitoylation in stabilizing nascent nicastrin and APH-1 polypeptides.

Our observation that *S*-palmitoylation deficiency results in the degradation of immature but not mature nicastrin raised the possibility that the *S*-palmitoylation-deficient mutants degrade before they exit the ER. To test this idea, we used the fungal metabolite brefeldin A (BFA), which perturbs membrane traffic at the ER-Golgi intersection by inducing Golgi disassembly. $NCT^{-/-}$ dWt and $NCT^{-/-}$ dMut cells were treated with BFA, and then analyzed by pulse-chase labeling in the presence of BFA. Lack of *S*-palmitoylation significantly increased the degradation of both nicastrin and APH-1 during the 8-h chase period even in the presence of BFA (Fig. 3*E*). To investigate whether the proteasome pathway is involved in the enhanced degradation of *S*-palmitoylation-deficient nicastrin and APH-1 in the ER, $NCT^{-/-}$ dWt, and $NCT^{-/-}$ dMut cells were treated with classic proteasome inhibitors. The steady-state levels of mutant APH-1 were markedly increased following 8 h treatment with lactacystin or MG132, whereas mutant immature nicastrin levels were only slightly increased (supplemental Fig. S4*A*). As expected, treatment of dWt and dMut with the lysosome inhibitor chloroquine exerted no effect on the steady-state levels of nicastrin and APH-1 mutants. Collectively, these data suggest that *S*-palmitoylation deficiency results in enhanced degradation of a subset of nascent APH-1 and nicastrin through the proteasome pathway.

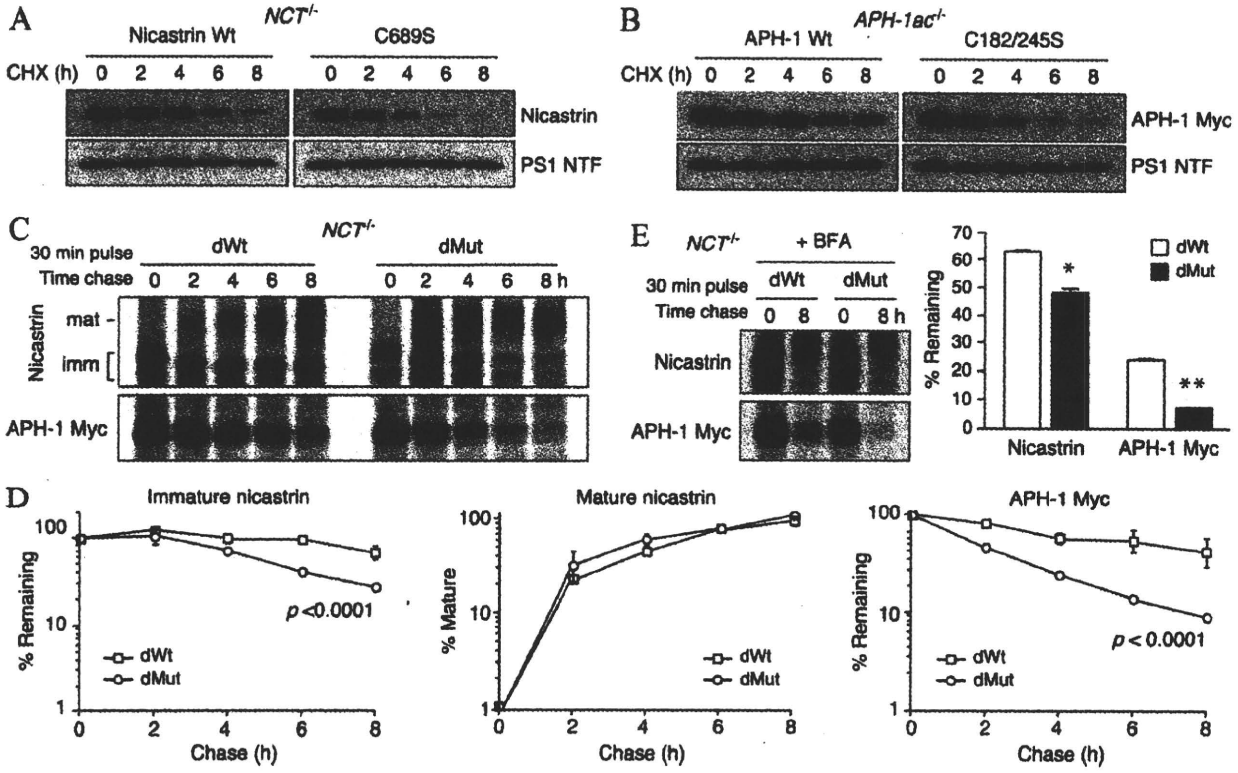

FIGURE 3. **S-Palmitoylation contributes to the stability of nascent nicastrin and APH-1.** *A* and *B*, lack of *S*-palmitoylation increases degradation of nicastrin and APH-1. $NCT^{-/-}$ pools expressing WT or C689S mutant (*A*), and *APH-1ac*$^{-/-}$ pools expressing WT or C142/285S mutant were incubated with CHX for various periods of time. The levels of nicastrin or APH-1, and PS1 remaining at the end of the incubation were analyzed by Western blotting using antibodies SP716, 9E10, and $PS1_{NT}$, respectively. *C*, pulse-chase analysis of protein stability. $NCT^{-/-}$ dWt and dMut MEF were pulse-labeled with 125 μCi/ml of [^{35}S]Met/Cys for 30 min and chased for the times indicated. Nicastrin and APH-1 were immunoprecipitated from aliquots of lysates at each time point using antibodies SP716 and 9E10, respectively (normalized to protein synthesis), and analyzed by SDS-PAGE and phosphorimaging. *D*, signal intensities were quantified and the protein levels remaining at each time point plotted relative to the level at time 0. The values represent mean ± S.E. of three experiments. Two-way analysis of variance comparison of data reveals statistically significant differences between the degradation of dWt and dMut. $p < 0.0001$. *E*, $NCT^{-/-}$ dWt and dMut MEF were pretreated with 5 μg/ml BFA and pulse-chase analysis was performed in the presence of BFA. Signal intensities from three experiments were quantified and the mean ± S.E. is plotted. *, $p < 0.05$; **, $p < 0.001$.

The impaired stability of nicastrin and APH-1 mutants led us to investigate whether *S*-palmitoylation deficiency increases ubiquitination of nicastrin and APH-1. To test this idea, we cotransfected an N-terminal His/Myc epitope-tagged ubiquitin (H_6M-Ub) with nicastrin and APH-1aL (tagged at the C terminus with the sequence SSRGPSSAEVLLLPVS) in HEK293 cells. Cell lysates were immunoprecipitated with antibodies against nicastrin or APH-1 and immunoprecipitates were subjected to immunoblotting with 9E10 antibody. The presence of H_6M-Ub on nicastrin and APH-1 was observed as a smear of high molecular weight species in the immunoprecipitates, which was enhanced by treatment of cells with the proteasome inhibitor lactacystin. Moreover, we found considerably greater levels of polyubiquitinated *S*-palmitoylation-deficient mutants as compared with WT nicastrin and APH-1. When the blots were reprobed, however, the high molecular weight signal was not detectable by antibodies against nicastrin or APH-1, indicating that only a small subset of these polypeptides undergo polyubiquitination (supplemental Fig. S4*B*). These data indicate that ubiquitin-mediated and ubiquitin-independent proteasome degradation pathways are involved in the degradation of a subset of *S*-palmitoylation-deficient nicastrin and APH-1.

S-Palmitoylation Is Required for DRM Association of Nicastrin and APH-1—*S*-Palmitoylation is an essential signal for lipid raft association of a large number soluble and integral membrane proteins (42). Lipid rafts are biochemically defined as detergent-resistant membrane domains that resist extraction with detergents such as Triton X-100 and Lubrol at 4 °C (43). Previously, we and others reported that all four γ-secretase subunits are present in DRM (13). Having established *S*-palmitoylation of two γ-secretase subunits, we examined the role of *S*-palmitoylation on DRM localization of γ-secretase subunits. We prepared membrane rafts from dWt and dMut $NCT^{-/-}$ MEF on the basis of detergent insolubility and low buoyant density on sucrose density gradients, essentially as described (13). Fractions enriched in DRM were identified by the enrichment of lipid raft marker, flotillin-2. We found a significant decrease (~70%) in the levels of *S*-palmitoylation-deficient nicastrin and APH-1 in the DRM fractions (Fig. 4, *A* and *B*). However, the absence of *S*-palmitoylation in nicastrin and APH-1 has only a minor effect on DRM localization of endogenous PS1 and PEN-2 (Fig. 4*A*). Further analysis by PS1 coimmunoprecipitation revealed reduced levels of PS1-bound nicastrin and APH-1 in DRM prepared from $NCT^{-/-}$ dMut

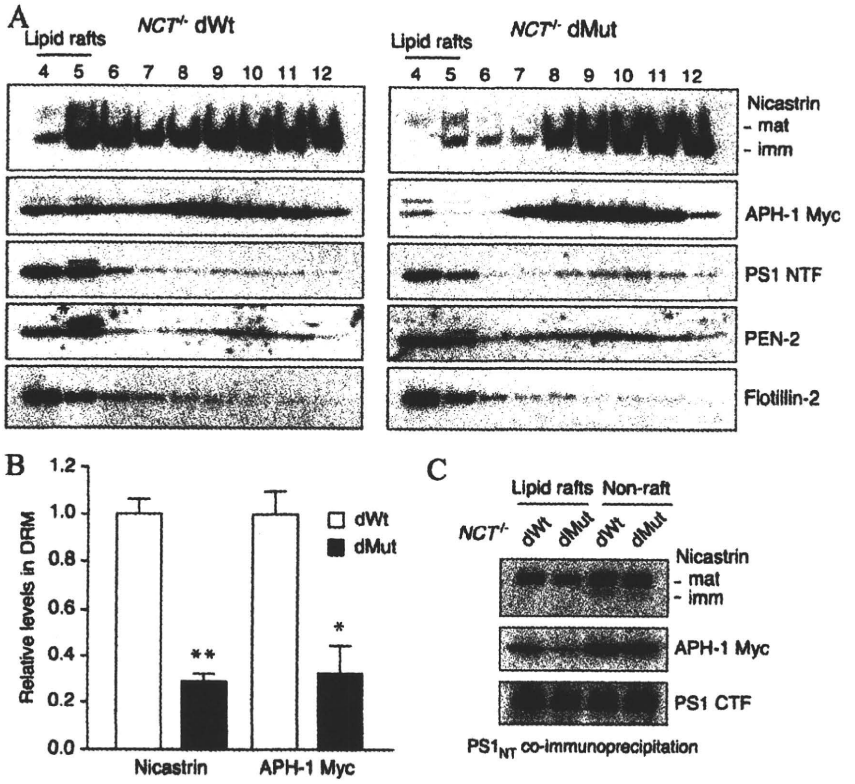

FIGURE 4. **S-Palmitoylation targets nicastrin and APH-1 to DRM.** *A*, $NCT^{-/-}$ dWt and dMut MEF were lysed in 0.5% Lubrol WX at 4 °C for 30 min. The lysates were then subjected to flotation centrifugation on discontinuous sucrose density gradients as described previously (13). Twelve 1-ml fractions were collected from the top and the distribution of γ-secretase subunits was determined by fractionating equal volume of fractions 4–12 followed by Western blotting using antibodies SP716, 9E10, $PS1_{NT}$, PNT2, and flotillin-2. Fractions 4 and 5 represent the interface between 5 and 35% sucrose in the gradient, and are enriched in the lipid raft marker flotillin-2. An *asterisk* indicates a nonspecific band observed in blots probed with PNT2. *B*, signal intensities of nicastrin and APH-1 in DRM fractions were quantified and the ratio of DRM (fractions 4 and 5) to total (signal in all fractions) signal was calculated for each experiment. The relative fold difference between dWt and dMut is plotted by normalizing WT ratios to 1. *, $p < 0.05$; **, $p < 0.01$. *C*, PS1 complexes in DRM were analyzed by co-immunoprecipitation using $PS1_{NT}$ antibody followed by immunoblotting using nicastrin and 9E10 antibodies.

MEF (Fig. 4*C*). Our data demonstrate a requirement for palmitoylation to promote DRM association of nicastrin and APH-1.

S-Palmitoylation Does Not Regulate Aβ Production—Next, we examined the effects of *S*-palmitoylation on γ-secretase processing of APP. First, we investigated the effect of *S*-palmitoylation on Aβ production in independent $NCT^{-/-}$ MEF pools stably co-expressing WT or *S*-palmitoylation-deficient nicastrin and APH-1. We transiently overexpressed APPSwe by retroviral infection and examined APP processing by metabolic labeling. A short 15-min pulse labeling with [^{35}S]Met/Cys confirmed that APP synthesis was comparable in each dWt and dMut pool examined (Fig. 5*A*). Full-length APP and APP CTFs were then immunoprecipitated from the lysates of cells labeled with [^{35}S]Met/Cys for 3 h. We found that the levels of α- and β-CTFs were comparable between $NCT^{-/-}$ dWt and $NCT^{-/-}$ dMut cells (Fig. 5*A*). As expected, $NCT^{-/-}$ cells transduced with empty vectors accumulated much higher levels of APP CTFs because of the lack of γ-secretase activity (Fig. 5*A*, *lane 1*). To directly quantify the levels of Aβ secreted by dWt and dMut pools, we collected media conditioned by these cells and performed sandwich ELISA. The results show that media conditioned by $NCT^{-/-}$ Vector cells contain only negligible amounts of Aβ; the levels of both Aβ40 and Aβ42 were significantly higher in dWt and dMut pools. However, the results of ELISA analyses show no difference in the levels of A0β40 or Aβ42 in the conditioned media, suggesting that lack of *S*-palmitoylation of γ-secretase subunits did not affect γ-secretase processing of APP (Fig. 5*B*).

To confirm the above findings we co-expressed *S*-palmitoylation-deficient nicastrin and APH-1 in the mouse N2a neuroblastoma cell line Swe10, which overexpresses human APP695 harboring the Swedish double mutation (35). We generated four independent N2aSwe pools each stably co-expressing WT or *S*-palmitoylation-deficient human nicastrin and APH-1aL. Co-immunoprecipitation analysis revealed that endogenous PS1 is associated with similar levels of nicastrin and APH-1 in dWt and dMut N2aSwe pools (Fig. 6*A*). Further analysis using a human nicastrin-specific mAb A5226 confirmed that endogenous mouse PS1 complexes with human WT or mutant nicastrin. Similarly, probing of PS1 co-immunoprecipitates with a polyclonal APH-1 antibody revealed that Myc-tagged human WT or mutant APH-1 co-immunoprecipitated with mouse PS1, replacing endogenous APH-1 (Fig. 6*B*). These results document that exogenously expressed nicastrin and APH-1 incorporated with endogenous γ-secretase subunits PS1 and PEN-2 in dWt and dMut N2aSwe pools. Moreover, these findings indicate that overexpressed *S*-palmitoylation-deficient human nicastrin and APH-1aL can replace endogenous WT subunits.

We then performed [^{35}S]Met/Cys labeling experiments to examine APP metabolism and found that APP processing and Aβ production were not affected by *S*-palmitoylation deficiency in nicastrin and APH-1 (Fig. 6*C*). Furthermore, ELISA quantification confirmed similar levels of secreted Aβ40 and Aβ42 peptides in the media conditioned by dWt and dMut N2aSwe pools (Fig. 6*D*). To finally rule out the possibly that substoichiometric expression of the four γ-secretase subunits might potentially cause experimental artifacts in N2aSwe cells, we overexpressed all four γ-secretase subunits and generated N2aPAP dWt and dMut pools (Fig. 7*A*). [^{35}S]Met/Cys labeling studies revealed similar levels of APP CTFs and secreted Aβ peptides in control N2aPAP (overexpressing PS1 and PEN-2) and N2aPAP dWt and N2aPAP dMut pools. Incubation of parallel dishes with 10 nM Com-

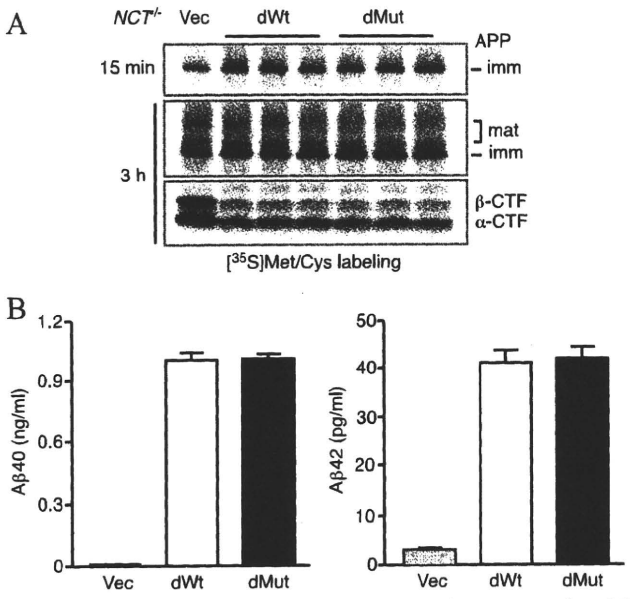

FIGURE 5. **S-Palmitoylation of nicastrin and APH-1 does not regulate Aβ production in $NCT^{-/-}$ MEF.** *A*, analysis of APP metabolism in stably transduced $NCT^{-/-}$ Vec, and three independent pools of dWt or dMut MEF. Cells were infected with APPSwe and labeled for 15 min or 3 h with 125 μCi/ml of [^{35}S]Met/Cys. Full-length APP and APP CTFs were immunoprecipitated from cell lysates using CTM1 antiserum. *B*, secreted Aβ40 and Aβ42 in the media conditioned by $NCT^{-/-}$ MEF expressing APPSwe were quantified using two-site ELISAs and normalized to the levels of secreted sAPPα.

pound E resulted in the accumulation of APP CTFs to similar levels, and marked (but incomplete) inhibition of Aβ secretion (Fig. 7*B*). Similarly, transient overexpression of mutant nicastrin and/or APH-1 failed to alter Aβ production in HeLa cells stably overexpressing APPSwe (supplemental Fig. S5). Collectively, these results demonstrate that deficiency in *S*-palmitoylation of γ-secretase does not affect amyloidogenic processing of APP.

S-Palmitoylation Does Not Modulate ε-Cleavage of APP, Notch, and N-cadherin—Next, we asked whether *S*-palmitoylation is necessary for γ-secretase cleavage of APP CTFs at the ε-site, which generates AICD. In these experiments, we infected cells with a C-terminal Myc-tagged APP CTF (APP C99-6Myc) and analyzed AICD generation by Western blotting and pulse-chase labeling. Because of the presence of C-Myc_6 tag, AICD generated by APP C99–6Myc has a longer half-life and is readily detectable in cell lysates. Western blot analysis of $NCT^{-/-}$ dWt and $NCT^{-/-}$ dMut MEF revealed comparable levels of AICD in cell lysates at steady-state (Fig. 8*A*). As expected, $NCT^{-/-}$ cells transduced with empty retrovirus vectors do not generate AICD. We then performed pulse-chase labeling studies to quantify AICD production and found no difference in the extent of APP C99 conversion to AICD between dWt and dMut cells (Fig. 8*B*). To confirm this finding using full-length APP, we prepared cell membranes from $NCT^{-/-}$ Vec, $NCT^{-/-}$ dWt, and $NCT^{-/-}$ dMut MEF transient overexpression of APPSwe, and performed *in vitro* AICD assays

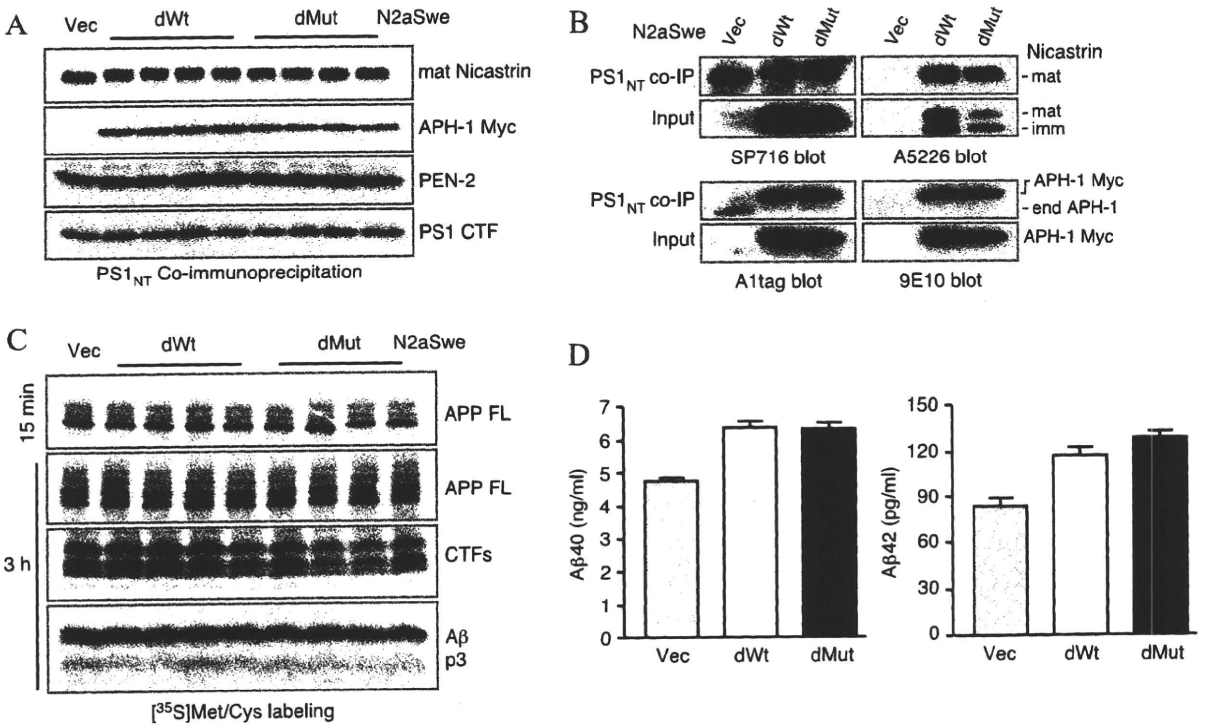

FIGURE 6. **S-Palmitoylation of nicastrin and APH-1 does not regulate Aβ production in N2a neuroblastoma cells.** *A* and *B*, co-immunoprecipitation (*IP*) analysis of PS1 complexes. *A*, independent stable pools of N2aSwe cells overexpressing WT nicastrin and APH-1 (N2aSwe dWt) or palmitoylation-defective nicastrin and APH-1 (N2aSwe dMut) were lysed in 1% CHAPSO buffer and analyzed by co-immunoprecipitation using $PS1_{NT}$ antibody. *B*, PS1 co-immunoprecipitates were analyzed by blotting with SP716 or A1tag antisera to detect endogenous and exogenous nicastrin and APH-1, respectively. The blots were reprobed with mAb A5226 or 9E10 to detect exogenous nicastrin and APH-1, respectively. *C*, analysis of APP metabolism. Stably transduced N2aSwe pools were labeled with [^{35}S]Met/Cys for 15 min or 3 h. Full-length APP and APP CTFs were immunoprecipitated from cell lysates with antibody CTM1. Aβ and p3 were immunoprecipitated from conditioned medium using mAb 4G8. *D*, secreted Aβ40 and Aβ42 were quantified from the conditioned media and normalized to the levels of sAPPα.

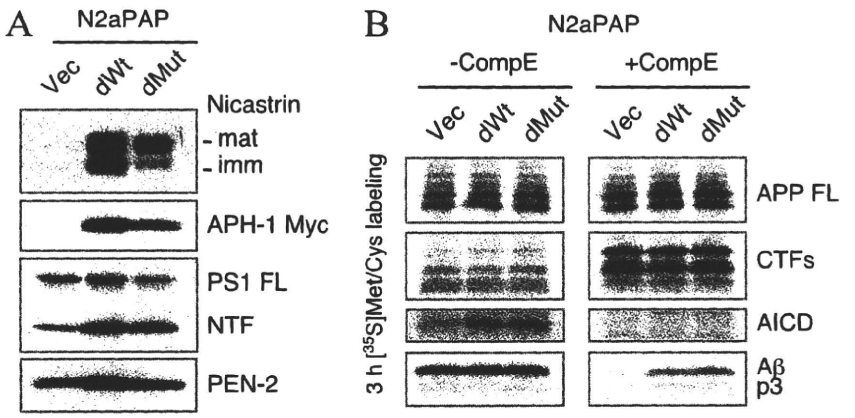

FIGURE 7. **Overexpression of *S*-palmitoylation-defective γ-secretase.** *A*, N2a cells stably overexpressing human WT PS1, APPSwe, and PEN-2 (*PAP*) were used to derive vector (*Vec*) or dWt and dMut pools (overexpressing nicastrin and APH-1). Expression of each γ-secretase subunit was analyzed by immunoblotting using antibodies SP716, 9E10, $PS1_{NT}$, and PNT2. *B*, PAP dWt and dMut cells were metabolically labeled with 125 μCi/ml of [^{35}S]Met/Cys for 3 h and analyzed as above. Parallel dishes were pretreated with 10 nM CompE overnight and labeled in the presence of CompE. Note that due to the overexpression of γ-secretase, treatment with 10 nM CompE resulted in partial inhibition of Aβ production, despite the complete inhibition of AICD production and marked accumulation of APP CTFs.

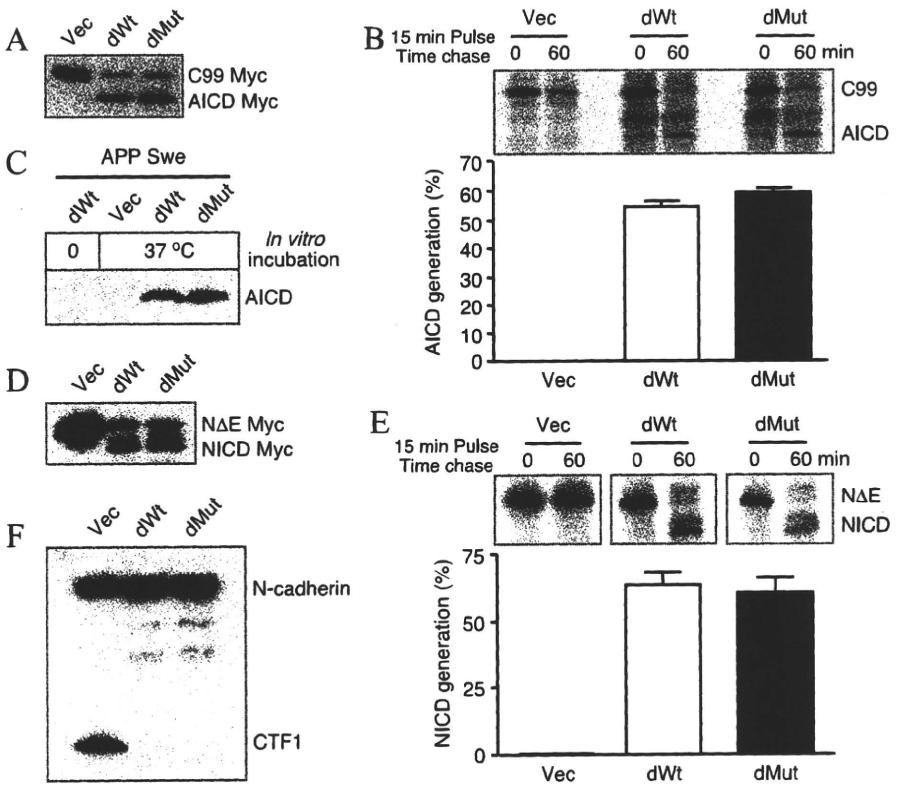

FIGURE 8. ***S*-Palmitoylation of nicastrin and APH-1 is not required for ε-cleavage.** *A*, the indicated $NCT^{-/-}$ pools were transiently infected with APP C99-6Myc and AICD generation was analyzed by immunoblotting with mAb 9E10. *B*, cells infected with C99-6Myc were pulse-labeled with 125 μCi/ml of [^{35}S]Met/Cys for 15 min and chased for 60 min. C99-6Myc and AICD-6Myc were immunoprecipitated from lysates using mAb 9E10 and the levels of AICD are plotted as percentage of C99-6Myc synthesis. Shown are the mean ± S.E. of three independent experiments. *C*, membranes were prepared from the indicated $NCT^{-/-}$ MEF transiently infected with APPSwe and incubated at 0 or 37 °C for 2 h to allow AICD generation. Supernatants containing AICD were analyzed by immunoblotting with mAb 9E10. *D*, $NCT^{-/-}$ pools were transiently infected with NotchΔEMV-6Myc and NICD production was assessed by immunoblotting. *E*, NICD production was quantified from three independent experiments by pulse-chase labeling as described above for AICD. *F*, lysates of $NCT^{-/-}$ MEF pools were analyzed by immunoblotting to assess γ-secretase cleavage of endogenous N-cadherin CTF1.

using established methods by incubating cell membranes prepared from these cells at 37 °C for 2 h to allow AICD generation (40). After centrifugation of the membranes, AICD released into supernatants were analyzed by Western blotting. We found that membranes from $NCT^{-/-}$ dWt and $NCT^{-/-}$ dMut MEF generate similar levels of AICD when incubated at 37 °C. As expected, membranes from cells $NCT^{-/-}$ Vector and $NCT^{-/-}$ dWt MEF reactions that were kept on ice failed to generate AICD (Fig. 8*C*). We also examined AICD production in intact cells. Overexpression of all γ-secretase subunits increased the levels of AICD in the lysates of N2aPAP dWt cells, as previously described (44). Consistent with the data from *in vitro* studies described above, we found similar levels of AICD were in lysates of N2aPAP dWt and dMut cells (Fig. 7*B*). Collectively, these results suggested that *S*-palmitoylation does not regulate ε-site cleavage of APP.

In addition to APP processing, γ-secretase cleavage of Notch receptor at the "ε-site" releases the Notch intracellular domain (NICD) (45–47). We examined whether *S*-palmitoylation of nicastrin and APH-1 affects Notch processing by γ-secretase, using the well characterized substrate NotchΔEMV-6Myc (31). Stable $NCT^{-/-}$ MEF pools were infected with NotchΔEMV-6Myc and analyzed by immunoblotting. As expected, the $NCT^{-/-}$ Vector pool does not generate NICD (Fig. 8*D*, *lane 1*). Compared with the $NCT^{-/-}$ fibroblast overexpressing WT nicastrin and APH-1, those overexpressing mutant nicastrin and APH-1 generated similar levels of NICD (Fig. 8*D*). We then pulse-labeled cells with [^{35}S]Met/Cys for 15 min and chased the cells for 60 min to quantify NICD generation, and found that $NCT^{-/-}$ dWt and dMut cells processed NotchΔEMV-6Myc precursor to NICD with similar efficiency (Fig. 8*E*). Finally, we assessed γ-secretase-mediated ε-cleavage of 40-kDa N-cadherin CTF1, which results in the production of a soluble intracellular

domain, termed N-cadherin CTF2 (48). In $NCT^{-/-}$ MEF endogenous N-cadherin CTF1 accumulates to high levels due to the absence of functional γ-secretase activity. We found that CTF1 generated from endogenous N-cadherin does not accumulate in either $NCT^{-/-}$ dWt or dMut MEF (Fig. 8*F*), indicating that lack of γ-secretase *S*-palmitoylation does not affect ε-cleavage of N-cadherin. These findings were confirmed by incubating dWt and dMut cells with varying concentrations of L685,458 or CompE, two highly selective γ-secretase inhibitors (supplemental Fig. S7). Thus, we conclude that *S*-palmitoylation of nicastrin and APH-1 has no effect on ε-site cleavage of γ-secretase substrates.

DISCUSSION

Over the past decade γ-secretase has been under greater scrutiny because of its essential role in the production of Aβ peptides and intramembrane proteolysis of numerous other transmembrane substrates. In the present study, we have identified and characterized a novel post-translational modification of two γ-secretase subunits. By direct metabolic labeling and a highly sensitive acyl thiol exchange labeling method (39), we demonstrate that nicastrin and APH-1 undergo *S*-palmitoylation in cultured cells and in the brain. The single *S*-palmitoylation site of nicastrin Cys^{689}, is conserved form *C. elegans* to human, whereas the *S*-palmitoylated APH-1 residues Cys^{182} and Cys^{245} are conserved in all three APH-1 isoforms expressed in mouse and human. By expression of *S*-palmitoylation-deficient nicastrin and APH-1 in $NCT^{-/-}$ and $APH\text{-}1ac^{-/-}$ MEF, respectively, we show that this modification is not essential for γ-secretase complex formation. Nevertheless, *S*-palmitoylation contributes to nascent polypeptide stability and DRM association of nicastrin and APH-1. By detailed examination of MEF and N2a cells stably co-expressing *S*-palmitoylation-deficient nicastrin and APH-1, we rule out a functional role of *S*-palmitoylation in γ-secretase processing of APP, Notch, and N-cadherin. Based on these findings, we conclude that *S*-palmitoylation plays a role in stability and raft localization of nicastrin and APH-1, but does not directly modulate γ-secretase processing of substrates.

Several functions have been ascribed to protein *S*-palmitoylation. In many cases, the presence of palmitate on proteins affects intracellular trafficking, association with cholesterol-rich membrane rafts, protein-protein interaction, and signaling functions (42). We used $NCT^{-/-}$ and $APH\text{-}1ac^{-/-}$ MEF to assess the role of *S*-palmitoylation in the formation of stable multiprotein enzyme complexes. Lack of either nicastrin or APH-1 destabilizes the remaining γ-secretase subunits resulting in marked diminution of their steady-state levels (reviewed in Ref. 10). Re-expression of WT or *S*-palmitoylation-deficient nicastrin and APH-1 in the respective knock-out MEF restored this defect. Data from co-immunoprecipitation analysis using an antibody against PS1 demonstrates that deficiency in *S*-palmitoylation does not affect γ-secretase subunit interactions that lead to the formation of stable complexes. Furthermore, when overexpressed in MEF and N2a cells *S*-palmitoylation-deficient human nicastrin and APH-1aL assembled with endogenous PS1 and PEN-2 to form γ-secretase complexes, thus acting as dominant mutants by replacing endogenous WT mouse nicastrin and APH-1 (Figs. 2 and 6).

Post-translational *S*-palmitoylation appears to confer stability to the target protein in many cases (reviewed in Ref. 17). In agreement, our pulse-chase labeling experiments reveal that *S*-palmitoylation contributes to the stability of nascent nicastrin and APH-1 polypeptides. One proposed mechanism by which *S*-palmitoylation alters protein stability involves shielding target proteins from proteasomal degradation, in some cases by blocking their ubiquitination. For example, palmitoylation contributes to the stability of cation-dependent mannose 6-phosphate receptor by masking a sorting signal; palmitoylation-defective mutant receptors are degraded by the proteasome following exit from the Golgi apparatus (49). Similarly, linker for activation of T cells mutant lacking palmitoylation is unstable and susceptible to degradation via the proteasome pathway (50). In the case of *S. cerevisiae* SNARE Tlg1 lack of palmitoylation results in ubiquitination and mislocalization to the vacuole for degradation (51). Consistent with the above idea, proteasomal inhibition by lactacystin and MG-132 partially stabilized *S*-palmitoylation-deficient APH-1aL and nicastrin, whereas the lysosome inhibitor chloroquine had no protective effect (supplemental Fig. S4*A*). Interestingly, a lysine residue is located three residues away from the *S*-palmitoylated cysteine in nicastrin (^{689}CINAK), and lysine residues are also located adjacent to Cys^{182} and Cys^{245} in human APH-1 isoforms 1aS, 1b, and 1c (Fig. 1*F*). In addition, a cluster of three lysine residues located within the second cytosolic loop (^{92}KLLKK) is conserved in all APH-1 isoforms. The precise site(s) of ubiquitination in APH-1 has not been defined. Although these data implicate that a subset of palmitoylation-defective mutants are degraded via the proteasome pathway, experiments performed by co-expressing ubiquitin reveal only a minor role for polyubiquitination as the signal responsible for proteasomal targeting (supplemental Fig. S4*B*).

S-Palmitoylation of nicastrin can occur in the ER as evidenced by the modification of endogenous immature nicastrin $PS1^{-/-}/PS2^{-/-}$ embryonic stem cells (supplemental Fig. S3). Pulse-chase studies conducted in the presence of BFA strongly suggests that *S*-palmitoylation-defective mutants are susceptible for rapid degradation in the absence of ER exit and transit through the secretory pathway (Fig. 3). It is therefore tempting to speculate that *S*-palmitoylation protects nascent nicastrin and APH-1 from ER-associated degradation. Interestingly, in pulse-chase studies mature complex glycosylated WT and *S*-palmitoylation-defective nicastrin were found to have comparable stability. Because maturation of nicastrin requires interaction with other γ-secretase subunits (reviewed in Ref. 10), the likely scenario is that complex formation with PS1 and PEN-2 stabilizes *S*-palmitoylation-deficient nicastrin and APH-1. In support of this notion, similar levels of WT or mutant nicastrin and APH-1 can be co-immunoprecipitated from stably transduced fibroblasts and N2a cells using antibodies against PS1. The above data are also in agreement with multiprotein complex formation as a means of escaping ubiquitin-independent "default" proteasome degradation of unstructured nascent polypeptides by the core 20 S proteasome (52, 53). Together, these findings suggest that one important function of *S*-palmitoylation is to protect nascent nicastrin and APH-1

from proteasomal degradation until they interact with PS1 and PEN-2, during their assembly into γ-secretase complexes.

S-Palmitoylation has been demonstrated as essential modification for raft localization of numerous cytosolic and transmembrane proteins (25, 54, 55). Our DRM fractionation studies reveal that *S*-palmitoylation contributes to, but is not absolutely required for, raft association of nicastrin and APH-1 (Fig. 4). Lack of *S*-palmitoylation in either nicastrin or APH-1 alone does not affect raft association γ-secretase subunits (supplemental Fig. S6). Importantly, in knock-out MEF co-expression of *S*-palmitoylation-deficient nicastrin and APH-1 does not have a significant effect on DRM association of endogenous PS1 and PEN-2. Based on these findings, we suggest that *S*-palmitoylation might promote the targeting of the nicastrin-APH-1 subcomplex to lipid rafts. The presence of a stable nicastrin-APH-1 subcomplex has been demonstrated as an early intermediate formed during the assembly of γ-secretase (56, 57). We found that co-immunoprecipitation with antibodies against PS1 still isolates *S*-palmitoylation-defective nicastrin and APH-1 from lipid raft fractions (Fig. 4). These later findings imply the presence of additional dominant signals or interacting proteins that target the fully assembled γ-secretase complex to rafts. Alternatively, when PS1 and PEN-2 assemble with *S*-palmitoylation-defective nicastrin and APH-1 subcomplex in non-raft domains, the fully assembled γ-secretase complexes would attract cholesterol and sphingolipids to create *de novo* raft microdomains around them. Further investigations are necessary to gain more information on γ-secretase association with lipid rafts.

We conducted detailed investigations to determine the functional importance of subunit *S*-palmitoylation on γ-secretase processing of substrates. $NCT^{-/-}$ MEF were initially used to readily assess gain of Aβ production upon expression of WT or mutant subunits. N2a neuroblastoma cells were used to accurately quantify Aβ40 and Aβ42 peptides, and to assess APP processing following overexpression of all four integral γ-secretase subunits. Results from metabolic labeling and ELISA analyses show that overexpression of *S*-palmitoylation-deficient nicastrin and APH-1 in $NCT^{-/-}$ MEF and N2aSwe does not affect Aβ40 or Aβ42 production. Moreover, *S*-palmitoylation of nicastrin and APH-1 had no effect on AICD generation in cultured cells as well as *in vitro* γ-secretase assays performed using purified cell membranes. Thus, our results clearly demonstrate that *S*-palmitoylation is not required for amyloidogenic processing of APP by γ-secretase in cultured cells. In addition to APP, we also analyzed γ-secretase processing of two additional substrates, Notch and N-cadherin. Here again, we found that lack of *S*-palmitoylation on nicastrin and APH-1 had no effect on intramembrane proteolysis of Notch and N-cadherin. Taken together, it is evident that *S*-palmitoylation of nicastrin and APH-1 is not essential for γ- and ε-site cleavage of substrates.

How do we reconcile the marked effect of *S*-palmitoylation on nascent nicastrin and APH-1 polypeptide stability with the observation that neither PS1 complex formation nor γ-secretase activity is impaired by the expression of mutant subunits? We suggest that in the culture systems employed in this investigation, overexpression of nicastrin and APH-1 is sufficient to overcome protein instability associated with lack of *S*-palmitoylation. Thus, despite nascent polypeptide instability protein overexpression drives the formation of PS1 complexes, allowing us to determine that *S*-palmitoylation does not directly contribute to substrate recognition or proteolysis. Nevertheless, to fully understand the physiological role of γ-secretase *S*-palmitoylation, it may be necessary to generate mouse models where the palmitoylation site mutations are introduced into *NCSTN* and *APH1* alleles by knock-in strategy. The roles of *S*-palmitoylation in γ-secretase trafficking and intramembranous cleavage of APP and other substrates in neurons and transgenic mice remain to be investigated.

Acknowledgments—We thank Dr. Guojun Bu for suggesting the use of BFA. We thank Drs. Yueming Li and Todd Golde for providing the γ-secretase inhibitors L685,458 and CompE, respectively.

REFERENCES

1. Selkoe, D. J. (2001) *Physiol. Rev.* **81,** 741–766
2. Sisodia, S. S., and St. George-Hyslop, P. H. (2002) *Nat. Rev. Neurosci.* **3,** 281–290
3. Iwatsubo, T. (2004) *Curr. Opin. Neurobiol.* **14,** 379–383
4. Thinakaran, G., Borchelt, D. R., Lee, M. K., Slunt, H. H., Spitzer, L., Kim, G., Ratovitsky, T., Davenport, F., Nordstedt, C., Seeger, M., Hardy, J., Levey, A. I., Gandy, S. E., Jenkins, N. A., Copeland, N. G., Price, D. L., and Sisodia, S. S. (1996) *Neuron* **17,** 181–190
5. Shah, S., Lee, S. F., Tabuchi, K., Hao, Y. H., Yu, C., LaPlant, Q., Ball, H., Dann, C. E., 3rd, Sudhof, T., and Yu, G. (2005) *Cell* **122,** 435–447
6. Chavez-Gutierrez, L., Tolia, A., Maes, E., Li, T., Wong, P. C., and de Strooper, B. (2008) *J. Biol. Chem.* **283,** 20096–20105
7. Francis, R., McGrath, G., Zhang, J., Ruddy, D. A., Sym, M., Apfeld, J., Nicoll, M., Maxwell, M., Hai, B., Ellis, M. C., Parks, A. L., Xu, W., Li, J., Gurney, M., Myers, R. L., Himes, C. S., Hiebsch, R., Ruble, C., Nye, J. S., and Curtis, D. (2002) *Dev. Cell* **3,** 85–97
8. Chen, F., Hasegawa, H., Schmitt-Ulms, G., Kawarai, T., Bohm, C., Katayama, T., Gu, Y., Sanjo, N., Glista, M., Rogaeva, E., Wakutani, Y., Pardossi-Piquard, R., Ruan, X., Tandon, A., Checler, F., Marambaud, P., Hansen, K., Westaway, D., St. George-Hyslop, P., and Fraser, P. (2006) *Nature* **440,** 1208–1212
9. Vetrivel, K. S., Gong, P., Bowen, J. W., Cheng, H., Chen, Y., Carter, M., Nguyen, P. D., Placanica, L., Wieland, F. T., Li, Y. M., Kounnas, M. Z., and Thinakaran, G. (2007) *Mol. Neurodegener.* 2:4
10. Vetrivel, K. S., Zhang, Y. W., Xu, H., and Thinakaran, G. (2006) *Mol. Neurodegener.* 1:4
11. Cordy, J. M., Hooper, N. M., and Turner, A. J. (2006) *Mol. Membr. Biol.* **23,** 111–122
12. Cheng, H., Vetrivel, K. S., Gong, P., Meckler, X., Parent, A., and Thinakaran, G. (2007) *Nat. Clin. Pract. Neurol.* **3,** 374–382
13. Vetrivel, K. S., Cheng, H., Lin, W., Sakurai, T., Li, T., Nukina, N., Wong, P. C., Xu, H., and Thinakaran, G. (2004) *J. Biol. Chem.* **279,** 44945–44954
14. Vetrivel, K. S., Cheng, H., Kim, S. H., Chen, Y., Barnes, N. Y., Parent, A. T., Sisodia, S. S., and Thinakaran, G. (2005) *J. Biol. Chem.* **280,** 25892–25900
15. Yang, X., Kovalenko, O. V., Tang, W., Claas, C., Stipp, C. S., and Hemler, M. E. (2004) *J. Cell Biol.* **167,** 1231–1240
16. Drenan, R. M., Doupnik, C. A., Boyle, M. P., Muglia, L. J., Huettner, J. E., Linder, M. E., and Blumer, K. J. (2005) *J. Cell Biol.* **169,** 623–633
17. Linder, M. E., and Deschenes, R. J. (2007) *Nat. Rev. Mol. Cell. Biol.* **8,** 74–84
18. Bijlmakers, M. J., and Marsh, M. (2003) *Trends Cell Biol.* **13,** 32–42
19. Topinka, J. R., and Bredt, D. S. (1998) *Neuron* **20,** 125–134
20. Hayashi, T., Rumbaugh, G., and Huganir, R. L. (2005) *Neuron* **47,** 709–723
21. Drisdel, R. C., Manzana, E., and Green, W. N. (2004) *J. Neurosci.* **24,** 10502–10510
22. Veit, M., Sollner, T. H., and Rothman, J. E. (1996) *FEBS Lett.* **385,** 119–123

23. Veit, M., Becher, A., and Ahnert-Hilger, G. (2000) *Mol. Cell Neurosci.* **15,** 408–416
24. Skene, J. H., and Virag, I. (1989) *J. Cell Biol.* **108,** 613–624
25. Takemoto-Kimura, S., Ageta-Ishihara, N., Nonaka, M., Adachi-Morishima, A., Mano, T., Okamura, M., Fujii, H., Fuse, T., Hoshino, M., Suzuki, S., Kojima, M., Mishina, M., Okuno, H., and Bito, H. (2007) *Neuron* **54,** 755–770
26. Benjannet, S., Elagoz, A., Wickham, L., Mamarbachi, M., Munzer, J. S., Basak, A., Lazure, C., Cromlish, J. A., Sisodia, S., Checler, F., Chretien, M., and Seidah, N. G. (2001) *J. Biol. Chem.* **276,** 10879–10887
27. Yanai, A., Huang, K., Kang, R., Singaraja, R. R., Arstikaitis, P., Gan, L., Orban, P. C., Mullard, A., Cowan, C. M., Raymond, L. A., Drisdel, R. C., Green, W. N., Ravikumar, B., Rubinsztein, D. C., El-Husseini, A., and Hayden, M. R. (2006) *Nat. Neurosci.* **9,** 824–831
28. Fukata, M., Fukata, Y., Adesnik, H., Nicoll, R. A., and Bredt, D. S. (2004) *Neuron* **44,** 987–996
29. Huang, K., Yanai, A., Kang, R., Arstikaitis, P., Singaraja, R. R., Metzler, M., Mullard, A., Haigh, B., Gauthier-Campbell, C., Gutekunst, C. A., Hayden, M. R., and El-Husseini, A. (2004) *Neuron* **44,** 977–986
30. Kitamura, T., Koshino, Y., Shibata, F., Oki, T., Nakajima, H., Nosaka, T., and Kumagai, H. (2003) *Exp. Hematol.* **31,** 1007–1014
31. Kopan, R., Schroeter, E. H., Weintraub, H., and Nye, J. S. (1996) *Proc. Natl. Acad. Sci. U. S. A.* **93,** 1683–1688
32. Hecimovic, S., Wang, J., Dolios, G., Martinez, M., Wang, R., and Goate, A. M. (2004) *Neurobiol. Dis.* **17,** 205–218
33. Ward, C. L., Omura, S., and Kopito, R. R. (1995) *Cell* **83,** 121–127
34. Sato, N., Urano, F., Leem, J. Y., Kim, S.-H., Li, M., Donoviel, D., Bernstein, A., Lee, A. S., Ron, D., Veselits, M. L., Sisodia, S. S., and Thinakaran, G. (2000) *Nat. Cell Biol.* **2,** 863–870
35. Thinakaran, G., Teplow, D. B., Siman, R., Greenberg, B., and Sisodia, S. S. (1996) *J. Biol. Chem.* **271,** 9390–9397
36. Thinakaran, G., Regard, J. B., Bouton, C. M. L., Harris, C. L., Price, D. L., Borchelt, D. R., and Sisodia, S. S. (1998) *Neurobiol. Dis.* **4,** 438–453
37. Leem, J. Y., Vijayan, S., Han, P., Cai, D., Machura, M., Lopes, K. O., Veselits, M. L., Xu, H., and Thinakaran, G. (2002) *J. Biol. Chem.* **277,** 19236–19240
38. Ogura, T., Mio, K., Hayashi, I., Miyashita, H., Fukuda, R., Kopan, R., Kodama, T., Hamakubo, T., Iwatsubo, T., Tomita, T., and Sato, C. (2006) *Biochem. Biophys. Res. Commun.* **343,** 525–534
39. Drisdel, R. C., and Green, W. N. (2004) *BioTechniques* **36,** 276–285
40. Tesco, G., Ginestroni, A., Hiltunen, M., Kim, M., Dolios, G., Hyman, B. T., Wang, R., Berezovska, O., and Tanzi, R. E. (2005) *J. Neurochem.* **95,** 446–456
41. Saura, C. A., Tomita, T., Davenport, F., Harris, C. L., Iwatsubo, T., and Thinakaran, G. (1999) *J. Biol. Chem.* **274,** 13818–13823
42. Smotrys, J. E., and Linder, M. E. (2004) *Annu. Rev. Biochem.* **73,** 559–587
43. Brown, D. A., and London, E. (1998) *Annu. Rev. Cell Dev. Biol.* **14,** 111–136
44. Kim, S. H., and Sisodia, S. S. (2005) *J. Biol. Chem.* **280,** 41953–41966
45. De Strooper, B., Annaert, W., Cupers, P., Saftig, P., Craessaerts, K., Mumm, J. S., Schroeter, E. H., Schrijvers, V., Wolfe, M. S., Ray, W. J., Goate, A., and Kopan, R. (1999) *Nature* **398,** 518–522
46. Struhl, G., and Greenwald, I. (1999) *Nature* **398,** 522–525
47. Mumm, J. S., Schroeter, E. H., Saxena, M. T., Griesemer, A., Tian, X., Pan, D. J., Ray, W. J., and Kopan, R. (2000) *Mol. Cell* **5,** 197–206
48. Georgakopoulos, A., Marambaud, P., Efthimiopoulos, S., Shioi, J., Cui, W., Li, H. C., Schutte, M., Gordon, R., Holstein, G. R., Martinelli, G., Mehta, P., Friedrich, V. L., Jr., and Robakis, N. K. (1999) *Mol. Cell* **4,** 893–902
49. Breuer, P., and Braulke, T. (1998) *J. Biol. Chem.* **273,** 33254–33258
50. Tanimura, N., Saitoh, S., Kawano, S., Kosugi, A., and Miyake, K. (2006) *Biochem. Biophys. Res. Commun.* **341,** 1177–1183
51. Valdez-Taubas, J., and Pelham, H. (2005) *EMBO J.* **24,** 2524–2532
52. Asher, G., Reuven, N., and Shaul, Y. (2006) *Bioessays* **28,** 844–849
53. Tsvetkov, P., Asher, G., Paz, A., Reuven, N., Sussman, J. L., Silman, I., and Shaul, Y. (2008) *Proteins* **70,** 1357–1366
54. Salaun, C., Gould, G. W., and Chamberlain, L. H. (2005) *J. Biol. Chem.* **280,** 19449–19453
55. Shogomori, H., Hammond, A. T., Ostermeyer-Fay, A. G., Barr, D. J., Feigenson, G. W., London, E., and Brown, D. A. (2005) *J. Biol. Chem.* **280,** 18931–18942
56. LaVoie, M. J., Fraering, P. C., Ostaszewski, B. L., Ye, W., Kimberly, W. T., Wolfe, M. S., and Selkoe, D. J. (2003) *J. Biol. Chem.* **278,** 37213–37222
57. Shirotani, K., Edbauer, D., Prokop, S., Haass, C., and Steiner, H. (2004) *J. Biol. Chem.* **279,** 41340–41345

Journal of Neurochemistry

JOURNAL OF NEUROCHEMISTRY | 2009 | 109 | 1648–1657

doi: 10.1111/j.1471-4159.2009.06069.x

A traditional medicinal herb *Paeonia suffruticosa* and its active constituent 1,2,3,4,6-penta-*O*-galloyl-β-D-glucopyranose have potent anti-aggregation effects on Alzheimer's amyloid β proteins *in vitro* and *in vivo*

Hironori Fujiwara,* Masahiro Tabuchi,† Takuji Yamaguchi,† Koh Iwasaki,* Katsutoshi Furukawa,‡ Kyoji Sekiguchi,† Yasushi Ikarashi,† Yukitsuka Kudo,§ Makoto Higuchi,¶,** Takaomi C. Saido,** Sumihiro Maeda,†† Akihiko Takashima,†† Masahiko Hara,‡‡ Nobuo Yaegashi,* Yoshio Kase† and Hiroyuki Arai‡

*Center for Asian Traditional Medicine, Tohoku University Graduate School of Medicine, Sendai, Aoba-ku, Japan

†TSUMURA Research Laboratories, TSUMURA & Co., Ibaraki, Japan

‡Department of Geriatrics and Gerontology, Division of Brain Sciences, Institute of Development, Aging and Cancer, Tohoku University, Aoba-ku, Sendai, Japan

§Innovation of Biomedical Engineering Center, Tohoku University, Aoba-ku, Sendai, Japan

¶Molecular Imaging Center, National Institute of Radiological Sciences, Inage-ku, Chiba, Japan

**Laboratory for Proteolytic Neuroscience, RIKEN Brain Science Institute, Wako, Saitama, Japan

††Laboratory for Alzheimer's Disease, RIKEN Brain Science Institute, Wako, Saitama, Japan

‡‡Local Spatio-Temporal Functions Laboratory, RIKEN Frontier Research System, Wako, Saitama, Japan

Abstract

The deposition of amyloid β (Aβ) protein is a consistent pathological hallmark of Alzheimer's disease (AD) brains; therefore, inhibition of Aβ fibril formation and destabilization of pre-formed Aβ fibrils is an attractive therapeutic and preventive strategy in the development of disease-modifying drugs for AD. This study demonstrated that *Paeonia suffruticosa*, a traditional medicinal herb, not only inhibited fibril formation of both $A\beta_{1-40}$ and $A\beta_{1-42}$ but it also destabilized pre-formed Aβ fibrils in a concentration-dependent manner. Memory function was examined using the passive-avoidance task followed by measurement of Aβ burden in the brains of Tg2576 transgenic mice. The herb improved long-term memory impairment in the transgenic mice and inhibited the accumulation of Aβ in the brain. Three-dimensional HPLC analysis revealed that a water extract of the herb contained several different chemical compounds including 1,2,3,4,6-penta-*O*-galloyl-β-D-glucopyranose (PGG). No obvious adverse/toxic were found following treatment with PGG. As was observed with *Paeonia suffruticosa*, PGG alone inhibited Aβ fibril formation and destabilized pre-formed Aβ fibrils *in vitro* and *in vivo*. Our results suggest that both *Paeonia suffruticosa* and its active constituent PGG have strong inhibitory effects on formation of Aβ fibrils *in vitro* and *in vivo*. PGG is likely to be a safe and promising lead compound in the development of disease-modifying drugs to prevent and/or cure AD.

Keywords: 1,2,3,4,6-penta-*O*-galloyl-β-D-glucopyranose, Alzheimer's disease, amyloid β protein, medicinal herb, *Paeonia suffruticosa*, Tg2576 transgenic mice.

J. Neurochem. (2009) **109**, 1648–1657.

Received November 27, 2008; revised manuscript received March 10, 2009; accepted March 23, 2009.

Address correspondence and reprint requests to Hiroyuki Arai, M.D., Ph.D., Department of Geriatrics and Gerontology, Division of Brain Sciences, Institute of Development, Aging and Cancer, Tohoku University, 4-1 Seiryo-cho Aobaku, Sendai 980-8575, Japan.
E-mail: harai@idac.tohoku.ac.jp

Abbreviations used: AD, Alzheimer's disease; APP, amyloid precursor protein; Aβ, amyloid β; MTT, 3-(4,5-dimethylthiazol-2-yl)-2,5-diphenyltetrazolium bromide; PGG, 1,2,3,4,6-penta-*O*-galloyl-β-D-glucopyranose.